**Universidade do Minho**
Escola de Medicina

Nuno Filipe Lopes dos Santos

# Targeting lactate transport for tumor immunotherapy

outubro de 2019

Nuno Filipe Lopes dos Santos **Targeting lactate transport for tumor immunotherapy**

UMinho|2019

The work presented in this thesis was performed in the Surgical Sciences Research Domain in the Life and Health Sciences Research Institute (ICVS), School of Medicine, University of Minho, Braga, Portugal (ICVS/3B'S-PT Government Associate Laboratory Braga/Guimarães, Portugal). Financial support was provided by FEDER funds through the Operational Programme Competitiveness Factors - COMPETE and National Funds through the Foundation for Science and Technology (FCT) - under the project POCI-01-0145-FEDER-007038; and by the project NORTE-01-0145-FEDER-000013, supported by Norte Portugal Regional Operational Programme (NORTE 2020), under the PORTUGAL 2020 Partnership Agreement, through the European Regional Development Fund (ERDF).

**Universidade do Minho**
Escola de Medicina

Nuno Filipe Lopes dos Santos

# Targeting lactate transport for tumor immunotherapy

Dissertação de Mestrado
Mestrado em Ciências da Saúde

Trabalho efetuado sob a orientação da
**Doutora Sara Costa Granja**
e da
**Doutora Sandra Maria Araújo da Costa**

outubro de 2019

## DIREITOS DE AUTOR E CONDIÇÕES DE UTILIZAÇÃO DO TRABALHO POR TERCEIROS

# AGRADECIMENTOS

À minha orientadora, Sara Granja, sem a qual eu não teria conseguido realizar este projeto. Obrigado por tudo, desde o momento em que entrei pela primeira vez no ICVS, muito antes de ter pensado em realizar este projeto. Introduziste-me ao mundo da ciência, ao mundo da investigação, aprendi tanta coisa contigo e tens estado sempre a apoiar-me mesmo nas situações mais complicadas em que duvidei de mim mesmo. Por toda a paciência e persistência, por saber que nem sempre foi fácil trabalhar comigo e mesmo assim não desististe, um enorme obrigado.

À minha coorientadora, Sandra Costa, obrigado por permitires que este trabalho fosse realizado da melhor maneira possível, por todas as sugestões, pela simpatia e também pelo enorme apoio prestado ao longo do ano, sobretudo nas situações mais complicadas.

À direção da Escola de Medicina da Universidade do Minho e do ICVS, obrigado pela oportunidade e por fornecer as condições necessárias para a realização deste trabalho nesta conceituada instituição, podendo assim contribuir para o avanço científico.

À minha colega de equipa na SG Team, Andreia, obrigado por todos os momentos de trabalho e de descontração no laboratório, por toda a ajuda que me deste ao longo deste ano e por estares sempre disponível independentemente das circunstâncias.

Às restantes pessoas do domínio das Ciências Cirúrgicas, Nathalia, Eduarda, Céline, Diana, Olga, Sónia, Raquel, Catarina Matos, Olívia, Sofia, entre outras, obrigado por tornarem cada dia no laboratório um dia diferente, por todo o conhecimento transmitido e por todo o apoio dado ao longo do ano.

Ao meu círculo mais fechado de amigos, Caroline, Marta, Joana, Bruna, Catarina e Sofia, por todos os dias terem estado ao meu lado durante esta "luta", que em conjunto se tornou mais fácil e permitiu que eu crescesse muito como pessoa e investigador, obrigado.

À minha namorada, Andreia Pinho, peça fundamental durante este ano, que esteve sempre ao meu lado e sempre soube lidar comigo da melhor forma. Conseguimos superar esta etapa juntos e tornou-nos mais fortes para o nosso futuro. Por nós, obrigado.

À minha família, por todo o incentivo, pela coragem e pelo amor e carinho que sempre me transmitiram. Este ano fez-me perceber que a família vem sempre em primeiro lugar e por terem estado sempre ao meu lado, obrigado.

# STATEMENT OF INTEGRITY

I hereby declare having conducted this academic work with integrity. I confirm that I have not used plagiarism or any form of undue use of information or falsification of results along the process leading to its elaboration.

I further declare that I have fully acknowledged the Code of Ethical Conduct of the University of Minho.

## O transporte de lactato como alvo para imunoterapia de tumores

O interesse no estudo do metabolismo das células tumorais tem vindo a aumentar devido a diversas evidências que demonstram que alterações no seu metabolismo celular dão origem a um microambiente tumoral acídico, através da libertação de lactato e protões pelos Transportadores de Monocarboxilato (MCTs), comprometendo a função das células imunes e assim potenciando o crescimento tumoral. Os MCTs são transportadores bidirecionais que medeiam o importe ou exporte de lactato dos vários tipos celulares presentes no microambiente tumoral. De facto, já foi demonstrado que o lactato pode modular a função dos macrófagos associados ao tumor (TAMs), um dos principais componentes celulares do microambiente tumoral, para um perfil anti-inflamatório. Assim sendo, neste estudo pretendemos investigar de que modo a inibição dos MCTs nas células tumorais ou nos TAMs leva a uma perturbação da relação metabólica existente entre estas populações, e consequentemente a uma redução do perfil imunossupressor dos TAMs. Neste trabalho, estudos de co-localização sugerem a existência de uma relação metabólica entre os TAMs e as células tumorais ao demonstrarem, em tumores subcutâneos de murganhos, a co-expressão de CD68, uma proteína expressa nos macrófagos, com a expressão do MCT2, uma isoforma responsável pelo importe de lactato, enquanto que a expressão do MCT4, isoforma responsável pelo exporte do lactato, foi detetada nas células tumorais. Posteriormente, inibimos o exporte de lactato nas células tumorais com o *knockout* (KO) do MCT1 e do MCT4. Verificamos que o KO do MCT1 aumentou a atividade glicolítica das células em concentrações baixas de glucose, mas não diminuiu a capacidade das células de exportarem lactato, assim como o KO do MCT4 não teve efeito na diminuição do exporte de lactato pelas células tumorais. Porém, em combinação com a inibição farmacológica do MCT1/2, levou a uma diminuição do exporte de lactato e da viabilidade celular. Apesar disso, o KO do MCT1 ou do MCT4 por si só não foi suficiente para modular o fenótipo dos macrófagos para um perfil pró-inflamatório. Curiosamente, quando inibimos a expressão do MCT2 nos macrófagos verificamos a diminuição da expressão de genes anti-inflamatórios e o aumento da expressão de genes pró-inflamatórios, indicando um papel crucial do MCT2 na relação metabólica entre células tumorais e macrófagos.

**Palavras-chave:** cancro; lactato; macrófagos; metabolismo; transportadores de monocarboxilatos

## Targeting lactate transport for tumor immunotherapy

Cancer cell metabolism has increasingly gained attention in the cancer research community, as studies demonstrated that metabolic reprogramming of cancer cells gives rise to an acidic microenvironment by the release of lactate and protons. The transport of lactate is done by the Monocarboxylate Transporters (MCTs) and this acidic microenvironment compromises the function of immune cells, helping tumor growth. Indeed, recent evidence have shown that lactate modulates tumor-associated macrophages (TAMs), a critical component of the tumor microenvironment (TME), towards an anti-inflammatory phenotype. MCTs are bidirectional transporters that play an important role in mediating the transport of lactate into and out of the different cell types of the tumor microenvironment. Therefore, we hypothesized that disrupting MCTs in cancer cells or in TAMs will interrupt this metabolic crosstalk and consequently control the immunosuppressive phenotype of TAMs. In this work, we demonstrated, in a murine Lewis lung carcinoma model, that expression of CD68, a glycoprotein expressed in macrophages, co-localized with the expression of MCT2, a known lactate importer, while MCT4, an isoform responsible for the export of lactate, was expressed in cancer cells, suggesting a metabolic crosstalk between TAMs and cancer cells. Therefore, we decided to disrupt lactate release from cancer cells by knocking out MCT1 and MCT4. MCT1 knockout (KO) increased the glycolytic activity of cells in low glucose conditions but was not able to decrease the export of lactate. MCT4 KO had no effect on decreasing lactate export, however, combination with pharmacological inhibition of MCT1/2 resulted in impaired lactate production and cell viability. Unfortunately, single MCT1 or MCT4 KO in cancer cells was not able to polarize macrophages towards a pro-inflammatory phenotype. On the other hand, MCT2 inhibition in macrophages resulted in a decrease in the expression of anti-inflammatory genes and an increase in the expression of pro-inflammatory genes, suggesting a crucial role of MCT2 in the metabolic crosstalk between cancer cells and macrophages.



**Keywords:** cancer; lactate; macrophages; metabolism; monocarboxylate transporters

# TABLE OF CONTENTS

**AGRADECIMENTOS** ..... **iii**

**LIST OF ABBREVIATIONS** ..... **ix**

**LIST OF FIGURES** ..... **xiii**

**LIST OF TABLES** ..... **xiv**

**CHAPTER 1 | INTRODUCTION** ..... **1**

1.1 Cancer epidemiology ..... 1

1.2 Cancer metabolism ..... 2

1.3 The impact of cancer metabolism in the microenvironment ..... 6

1.3.1 Tumor-associated macrophages ..... 7

1.4 Monocarboxylate transporters ..... 12

1.4.1 The role of MCTs in lactate shuttles ..... 13

1.4.2 MCTs as therapeutic targets ..... 16

**CHAPTER 2 | OBJECTIVES** ..... **18**

**CHAPTER 3 | MATERIALS AND METHODS** ..... **19**

3.1 Cell lines and cell culture ..... 19

3.2 Immunohistochemistry ..... 19

3.3 Immunofluorescence ..... 20

3.4 Generation of MCT1 and MCT4-null cells ..... 21

3.5 Western Blot ..... 21

3.6 Cell biomass analysis ..... 22

3.7 Glucose and lactate measurement ..... 23

3.8 Bone marrow-derived macrophages isolation ..... 23

3.9 Co-culture experiments ..... 24

3.10 RNA Extraction ..... 25

3.11 Complementary DNA (cDNA) synthesis ..... 25

3.12 Real-Time Quantitative Polymerase Chain Reaction (RT-qPCR) ..... 26
3.13 ELISA ..... 28
3.14 Small interfering RNA (siRNA) transfection ..... 29
3.15 Statistical analysis ..... 29
**CHAPTER 4 | RESULTS ..... 30**
4.1 Tumor-associated macrophages co-localized with MCT2 ..... 30
4.2 Generation and characterization of MCT1 KO breast cancer cells ..... 31
4.3 Generation and characterization of MCT4 KO breast cancer cells ..... 33
4.4 Single targeting MCT1/4 was not able to polarize macrophages towards a pro-inflammatory phenotype ..... 35
4.5 Targeting MCT2 inhibited the M2-like phenotype of macrophages ..... 37
**CHAPTER 5 | DISCUSSION ..... 39**
**CHAPTER 6 | CONCLUDING REMARKS AND FUTURE PERSPECTIVES ..... 45**
**CHAPTER 7 | BIBLIOGRAPHY ..... 46**

# LIST OF ABBREVIATIONS

3PG - 3-Phosphoglycerate

**A**

ATCC - American type culture collection

ATP - Adenosine triphosphate

**B**

BMDM - Bone marrow-derived macrophages

BSA - Bovine serum albumin

**C**

CAFs - Cancer-associated fibroblasts

Cas9 - CRISPR-associated protein 9

CD - Cluster of differentiation

cDMEM - Complete Dulbecco's Modified Eagle Medium

cDNA - Complementary DNA

CHC - α-cyano-4-hydroxy-cinnamate

CRISPR - Clustered Regularly Interspaced Short Palindromic Repeat

CSF1R - Colony stimulating factor 1 receptor

**D**

DAB - 3,3′-Diamonobenzidine

DAPI - 4′,6-diamidino-2-phenylindole

DC - Dendritic cells

DMEM - Dulbecco's Modified Eagle Medium

DNA - Deoxyribonucleic acid

DSB - Double stranded break

**E**

ECACC - European Collection of Authenticated Cell Cultures

ELISA - Enzyme-linked immunosorbent assay

EMT - Epithelial-to-mesenchymal transition

ETC - Electron transport chain

**F**

F6P - Fructose-6-phosphate

FACS - Fluorescence-activated cell sorting

FAO - Fatty acid oxidation

FBS - Fetal bovine serum

**G**

G6P - Glucose-6-phosphate

G6PDH - Glucose-6-phosphate dehydrogenase

GA3P - Glyceraldehyde-3-phosphate

GCO - Global Cancer Observatory

GFP - Green fluorescent protein

GLS - Glutaminase

GLUT - Glucose transporter

GM-CSF - Granulocyte-macrophage colony stimulating factor

GPR132 - G protein coupled-receptor 132

GS - Glutamine synthetase

**H**

HDR - Homology-directed repair

HEPES - 4-(2-hydroxyethyl)-1-piperazineethanesulfonic acid

HIF-1α - Hypoxia inducible factor 1-alpha

HK - Hexokinase

HRP - Horseradish peroxidase

**I**

IARC - International Agency for Research on Cancer

IDH - Isocitrate dehydrogenase

IL - Interleukin

iNOS - Inducible nitric oxide synthase

**K**

KO - Knockout

**L**

LCCM - L929-cell conditioned medium

LDH - Lactate dehydrogenase

LLC - Lewis lung carcinoma

LPS - Lipopolysaccharides

**M**

MCT - Monocarboxylate transporter

MDSCs - Myeloid-derived suppressor cells

MHC-II - Major Histocompatibility Complex II

MMPs - Matrix metalloproteinases

mTOR - Mammalian target of rapamycin

**N**

NADH - Nicotinamide adenine dinucleotide

NADPH - Nicotinamide adenine dinucleotide phosphate

NK - Natural killer cells

NO - Nitric Oxide

**O**

OAA - Oxaloacetate

OXPHOS - Oxidative phosphorylation

**P**

PBS - Phosphate-buffered saline

PFK1 - Phosphofructokinase 1

PKM2 - Pyruvate kinase isoform 2

PPP - Pentose phosphate pathway

**R**

REDD1 - Regulated in development and DNA damage response 1

RFP - Red fluorescent protein

Ribose-5P - Ribose-5-phosphate

RNA - Ribonucleic acid

ROS - Reactive oxygen species

RT-qPCR - Real-Time Quantitative Polymerase Chain Reaction

**S**

SDH - Succinate dehydrogenase

SDS-PAGE - Sodium dodecyl sulfate-polyacrylamide gel electrophoresis

shRNA - Short hairpin RNA

siRNA - Small interfering RNA

SLC16 - Solute carrier family 16

SRB - Sulforhodamine B

**T**

TAMs - Tumor-associated macrophages

TBS - Tris-buffered saline

TCA - Trichloroacetic acid

TCA cycle - Tricarboxylic acid cycle

TGF-β - Transforming growth factor-beta

TME - Tumor microenvironment

TNF-α - Tumor necrosis factor-alpha

Treg - Regulatory T cells

**U**

UICC - Union for International Cancer Control

**V**

VEGF - Vascular endothelial growth factor

α-KG - Alpha-ketoglutarate

# LIST OF FIGURES

Figure 1. Percentages of new cancer cases and cancer deaths worldwide in 2018, according to the IARC. ..... 1
Figure 2. Percentages of new cancer cases and cancer deaths in Portugal in 2018, according to the IARC. ..... 2
Figure 3. Representation of the metabolism in normal cells and the Warburg effect in cancer cells. ..... 3
Figure 4. Metabolic intermediates used in the biosynthetic pathways. ..... 4
Figure 5. Diagram of the glycolytic pathway. ..... 5
Figure 6. Functional plasticity of macrophages. ..... 8
Figure 7. M1-like macrophage metabolism ..... 9
Figure 8. M2-like macrophage metabolism. ..... 10
Figure 9. Lactate shuttle between glycolytic and oxidative cancer cells ..... 14
Figure 10. Lactate shuttle between cancer cells and endothelial cells. ..... 15
Figure 11. Lactate shuttle between oxidative cancer cells and stromal cells in the tumor microenvironment ..... 15
Figure 12. Shuttling of metabolites between cancer cells and immune cells. ..... 16
Figure 13. Tumor-associated macrophages co-localized with MCT2. ..... 30
Figure 14. Effect of MCT1 disruption in breast adenocarcinoma cell line E0771. ..... 32
Figure 15. Effect of MCT4 disruption in breast adenocarcinoma cell line E0771. ..... 34
Figure 16. Single targeting of MCT1/4 was not able to polarize macrophages towards a pro-inflammatory phenotype. ..... 36
Figure 17. Targeting MCT2 inhibits the M2-like phenotype of macrophages. ..... 38

# LIST OF TABLES

Table 1. Primary antibodies used in immunofluorescence analysis. ..... 20
Table 2. Secondary antibodies used in immunofluorescence analysis. ..... 20
Table 3. Primary antibodies used in Western blot. ..... 22
Table 4. Secondary antibodies used in Western blot. ..... 22
Table 5. Volumes of RT-qPCR mixture used per each sample in evaluating M1 and M2 gene expression. ..... 26
Table 6. RT-qPCR amplification program using ABI Prism 7500 (Applied Biosystems). ..... 26
Table 7. TaqMan™ probes used in RT-qPCR experiments. ..... 27
Table 8. Volumes of RT-qPCR mixture used per each sample in evaluating MCTs expression. ..... 27
Table 9. RT-qPCR amplification program using CFX96 Touch Real-Time PCR Detection System (Bio-Rad). ..... 28
Table 10. Sequence of the primers used in the RT-qPCR experiments. ..... 28

# CHAPTER 1 | INTRODUCTION

## 1.1 Cancer epidemiology

Cancer incidence and mortality are growing in every country of the world in the 21st century and, according to the World Health Organization, is the primary leading cause of death in 91 countries[1]. This is due to the growth and aging of the population and increased exposure to cancer risk factors, often associated with socioeconomic development. The GLOBOCAN 2018 database, produced by the International Agency for Research on Cancer (IARC), estimated 18.1 million new cancer cases and 9.6 million cancer deaths worldwide in 2018, with lung and breast cancer being the most frequently diagnosed cancers (11.6%). Lung cancer is also the main cause of cancer death worldwide (18.4%), followed by colorectal cancer (9.2%) (Figure 1)[2].

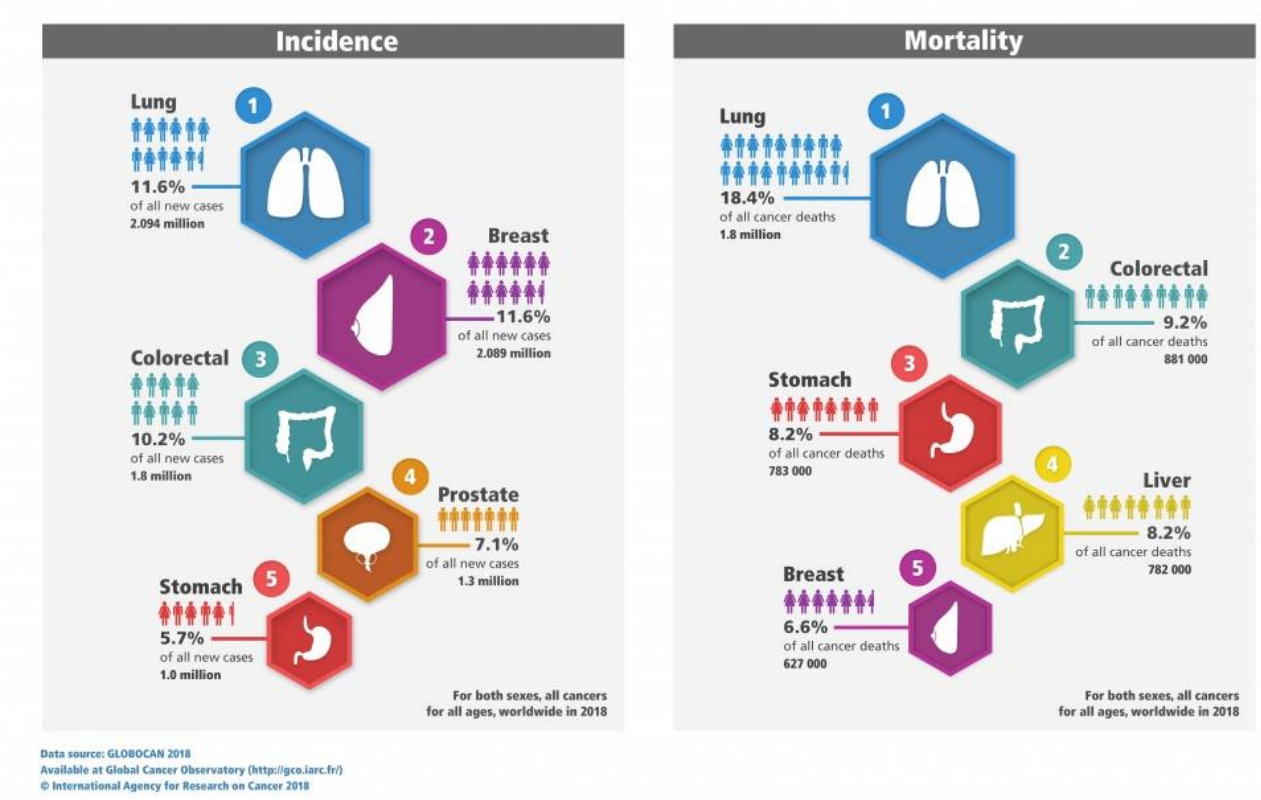


**Figure 1. Percentages of new cancer cases and cancer deaths worldwide in 2018, according to the IARC.** Adapted from Union for International Cancer Control (UICC) https://www.uicc.org/.

According to the GLOBOCAN database, colorectal cancer (17.6%) is the most commonly diagnosed cancer in Portugal, followed by breast cancer (12%), while lung cancer (16.1%) and colorectal cancer (14.7%) are the leading cause of cancer death (Figure 2)[2].

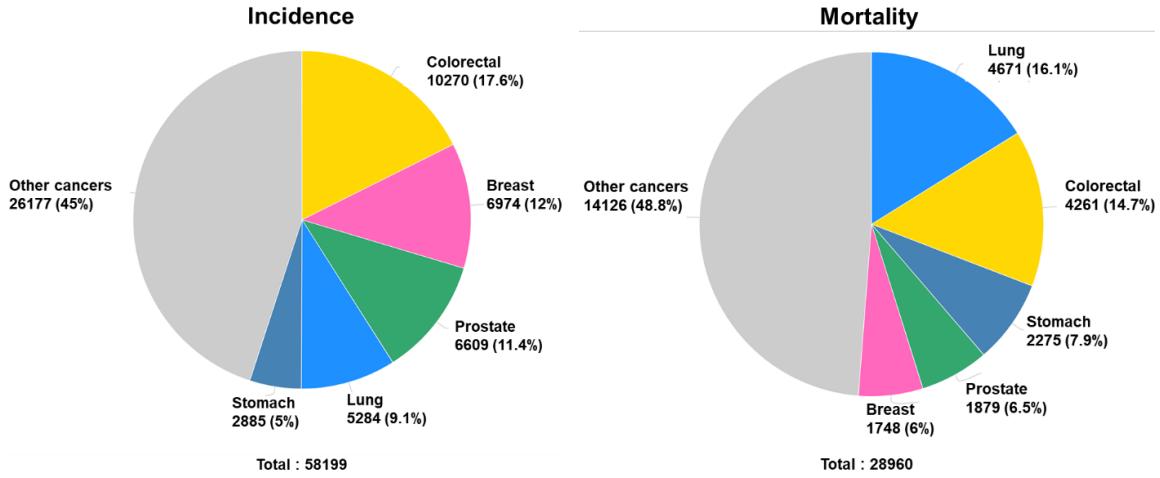


**Figure 2. Percentages of new cancer cases and cancer deaths in Portugal in 2018, according to the IARC.** Adapted from Global Cancer Observatory (GCO) http://www.gco.iarc.fr/.

## 1.2 Cancer metabolism

Cancer metabolism emerged as an area of extensive research in cancer biology, based on observations that metabolic activities are altered in cancer cells relative to non-cancerous cells, which supports the transformation of a cell into a neoplastic state. This field can also help to identify suitable therapeutic targets that are altered in cancer cells[3].

It is known that normal cells, in the presence of oxygen, convert glucose into pyruvate, which further enters the mitochondria for oxidative phosphorylation (OXPHOS), in order to generate adenosine triphosphate (ATP), essential for energy supply to cells. Meanwhile, under hypoxic conditions, pyruvate is converted into lactate (Figure 3)[4].

In the 1920s, Otto Warburg reported differences between the metabolic pathways of normal cells and cancer cells[5]. Unlike normal cells, cancer cells increase the rate of glucose consumption and have a preference to produce lactate, instead of performing OXPHOS in the mitochondria, regardless of oxygen availability (Figure 3). This observation that cancer cells rely on glycolysis to produce energy, even in the presence of oxygen, is known as the Warburg effect or aerobic glycolysis[6,7], and it is considered a hallmark of cancer cells[8].

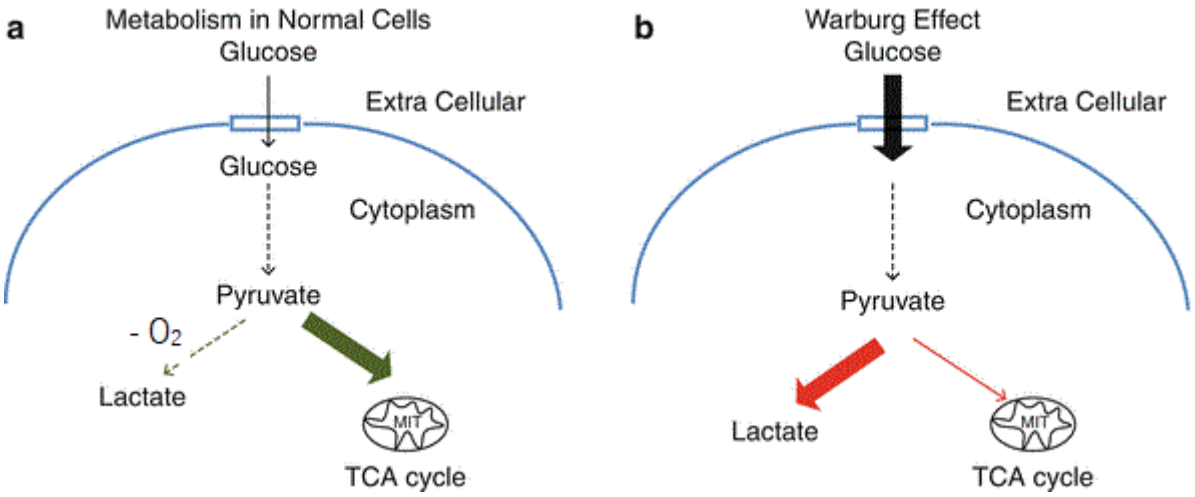


**Figure 3. Representation of the metabolism in normal cells and the Warburg effect in cancer cells. a)** Normal cells, in the presence of oxygen, convert glucose into pyruvate, which is oxidized through OXPHOS in the mitochondria. Under hypoxic conditions, pyruvate is reduced to lactate. **b)** Cancer cells demonstrate a preference to produce lactate, regardless of oxygen availability. Adapted from Venkatesh et al., 2013[183].

This highly glycolytic phenotype of cancer cells provides several advantages. Although OXPHOS has a higher ATP yield per molecule of glucose than glycolysis, glycolysis produces ATP at a faster rate, supplying immediate energy to support the metabolic demands of proliferating cells. Furthermore, the breakdown of glucose generates intermediate metabolites needed for biosynthetic pathways, such as the pentose phosphate pathway (PPP), that supports cell growth and proliferation. These metabolic intermediates can be synthesized into nucleotides, lipids or nonessential amino acids[9]. Like glycolytic intermediates, tricarboxylic acid (TCA) cycle intermediates are also used in the biosynthetic pathways (Figure 4)[10]. Moreover, the upregulation of glycolysis prevents cell death induced by reactive oxygen species (ROS) such as hydrogen peroxide[11,12].

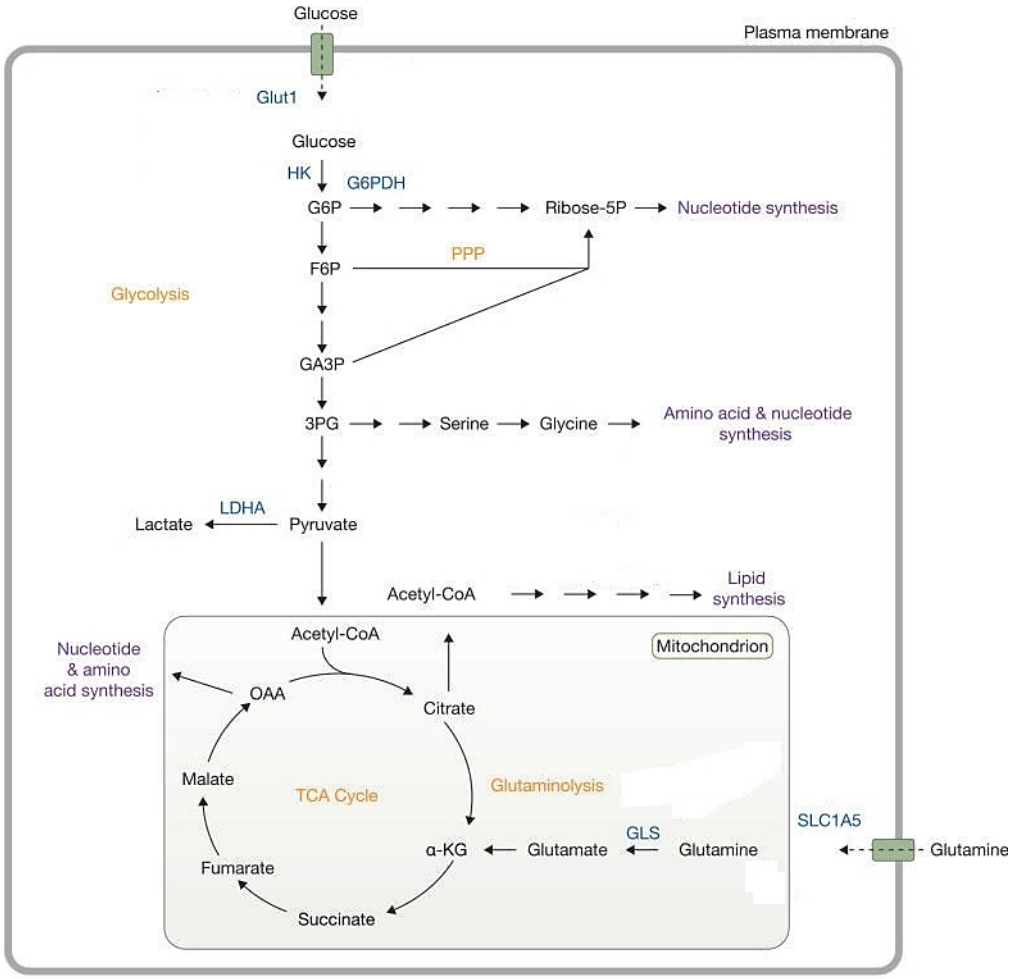


**Figure 4. Metabolic intermediates used in the biosynthetic pathways.** Glycolysis provides metabolic intermediates for biosynthetic pathways that support cancer cells growth and proliferation. Like glycolysis, glutamine catabolism provides TCA cycle intermediates that help cancer cells growth and proliferation. Glut1: glucose transporter 1; HK: hexokinase; G6P: glucose-6-phosphate; G6PDH: glucose-6-phosphate dehydrogenase; Ribose-5P: ribose-5-phosphate; PPP: pentose phosphate pathway; F6P: fructose-6-phosphate; GA3P: glyceraldehyde-3-phosphate; 3PG: 3-phosphoglycerate; LDHA: Lactate Dehydrogenase A; GLS: glutaminase; α-KG: alpha-ketoglutarate; OAA: oxaloacetate; SLC1A5: neutral amino acid transporter; TCA cycle: tricarboxylic acid cycle. Adapted from Boroughs and DeBerardinis, 2013[9].

The metabolic demands of proliferating cancer cells surpass the vasculature ability to provide oxygen and nutrients, resulting in a low-oxygen environment (hypoxia)[3]. Cancer cells present a metabolic response to hypoxic conditions by switching from OXPHOS to glycolytic pathway to generate ATP[13]. This metabolic adaption is mediated by the transcription factor hypoxia-inducible factor 1 alpha (HIF-1α), which induces the upregulation of glycolytic transporters and enzymes, such as glucose transporters GLUT1 and GLUT3, Hexokinase II (HK II), Pyruvate kinase isoform 2 (PKM2), Lactate Dehydrogenase A (LDH-A), among others[14–18]. Constitutive HIF-1α expression has also been reported under aerobic conditions, promoted by the glycolytic metabolism of cancer cells[19]. Cancer cells also upregulate the three rate-limiting enzymes of the glycolytic pathway, HK II, phosphofructiokinase1 (PFK1) and PKM2, to ensure an high glycolytic flux (Figure 5)[20].

Accumulation of pyruvate inside cancer cells can cause cell death[21], and in order to avoid it, cancer cells upregulate LDH-A, promoting the reduction of pyruvate into lactate to generate ATP and support cell proliferation[22–24]. Lactate dehydrogenases are responsible for the interconversion of pyruvate and lactate (Figure 5). LDH-A catalyzes the reduction of pyruvate into lactate as the final product of glycolysis, while LDH-B promotes the conversion of lactate into pyruvate[22]. Coupled with lactate production is the oxidation of nicotinamide adenine dinucleotide (NADH) into NAD+, a cofactor required to sustain glycolysis and therefore, ATP production[25,26]. High levels of LDH-A promote cancer cell epithelial to mesenchymal transition (EMT), angiogenesis, invasion and migration[27–29] and are correlated with poor prognosis in many human tumors[30–32].

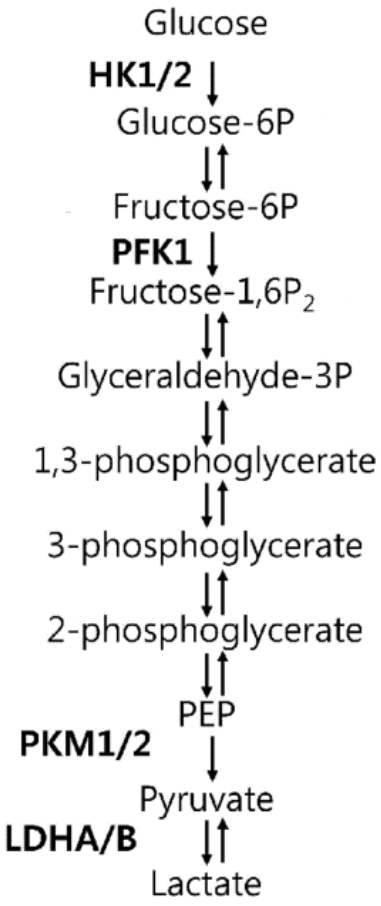


**Figure 5. Diagram of the glycolytic pathway.** Cancer cells upregulate the enzymes hexokinase (HK), phosphofructokinase 1 (PFK1), pyruvate kinase (PK) and lactate dehydrogenase A (LDH-A). The rate-limiting enzymes of glycolysis, along with lactate dehydrogenase are in bold. Adapted from Kim and Yeom, 2018[184].

## 1.3 The impact of cancer metabolism in the microenvironment

The tumor microenvironment (TME) is composed not only by proliferating cancer cells, but comprises a mass of heterogeneous cell types, including cancer and non-cancerous cells. Early studies solely focused in cancer cells to explain tumor growth, however, thanks to remarkable progress in cancer research, the TME is now recognized as an active participant in the tumorigenesis, supporting tumor growth[8].

The first association between inflammation and cancer was documented in 1863 by Rudolf Virchow when he detected leukocytes in tumor tissues and made the connection between cancer and inflammation[33]. This observation gained significant attention in the last few years, leading to the recognition of the tumor-associated inflammation as a key hallmark of cancer[8]. Inflammation is characterized by a complex biological response to cellular damage, where the immune system attempts to eliminate and neutralize the injury and initiate the regenerative and healing processes[34]. Immune cell activation leads to important alterations in several signaling pathways in order to exert their effector function. This process is metabolically challenging and therefore, immune cells reprogram their metabolism to sustain their energetic and metabolic needs[35–37]. In the last few years, immunometabolism has become one of the most exciting areas of translational research, allowing to understand how metabolic pathways determine specific immune cell fate and the functional responses, which is crucial to perceive and target cancer immune evasion, a hallmark of cancer cells[8,38].

The glycolysis end-product lactate is an essential metabolite that circulates at levels of 1-2 mM and acts as an inter-organ carbon shuttle in mammals[39,40], rising to 10 mM and even to 30-40mM in the TME[41]. Lactate has also been greatly associated with cancer aggressiveness and poor survival[42,43]. Lactate contributes to several features of tumor progression, including cell migration and invasion, angiogenesis and escape to immune surveillance[44–47]. As a feature of high glycolytic flux, cancer cells symport lactate and protons to the extracellular environment to avoid glycolysis inhibition due to a negative feedback mechanism and also to maintain the pH homeostasis[48]. The accumulation of lactate and protons in the extracellular space induces a drop in the extracellular pH, acidifying the TME[49,50]. The discovery of an acidic pH in tumor sites raised questions as to whether lactate could have effects on cellular metabolism that might contribute to the modulation of immune cell function during inflammation in the TME. Evidence indicates that high levels of extracellular lactate directly influence immune cell metabolism and cytokine production and may serve as a negative feedback signal, limiting inflammation[51–55].

Extracellular acidification reduced the export of lactate by monocytes and macrophages, impairing glycolysis and consequently the expression of pro-inflammatory mediators[36,56]. Lactate inhibited monocytes differentiation to dendritic cells (DC) and decreases cytokine release[57]. In a murine glioma model, treatment with diclofenac, a LDH-A inhibitor, reduced intratumoral lactate levels that resulted in the reactivation of DC, which inhibited accumulation and activation of regulatory T cells (Treg)[58]. LDH-A knockdown in pancreatic cancer cells decreased the number of myeloid-derived suppressor cells (MDSCs) in the tumor niche[54]. Tumor-derived lactate promoted MDSCs proliferation and survival[59]. High concentrations of lactate in the extracellular medium inhibited the export of lactate by activated T cells, thereby disturbing their metabolism and function[60]. Furthermore, lactate suppressed the proliferation and cytokine production of cytotoxic T cells[60,61]. However, neutralizing the extracellular pH abrogated the effect of lactate[62]. This demonstrates that acidification of the medium synergizes with lactate to promote an immunosuppressive environment. In addition, tumor-derived lactate promoted naive T cells apoptosis, autophagy impairment and consequently, poor anti-tumor immunity[63]. The acidic tumor microenvironment is permissive for the accumulation of Treg cells, as their frequency in tumor sites often correlates with poor prognosis in several cancers. The inhibition of glycolysis, as a consequence of high levels of extracellular lactate, increased the expression of transcription factor FoxP3, an important transcription factor for Treg cell function[61]. FoxP3 stimulates the oxidation of extracellular lactate to fuel mitochondrial activity, providing Treg cells with a metabolic advantage in high-lactate conditions[64]. This adaptation of Treg cells to acidic conditions potentiates their immune suppressive function.

Previously considered as a waste product of cancer metabolism, lactate represents an important signaling molecule involved in sophisticated mechanisms that shutdown anti-tumor immune responses and activate potent negative regulators of innate and adaptive immunity[65].

### 1.3.1 Tumor-associated macrophages

Among immune cells, macrophages were the first cells to be described in human tumors[66] and can comprise up to half of the tumor-infiltrating immune cells, where they become tumor-associated macrophages (TAMs)[67]. Macrophages are known to present high functional plasticity, with the ability to express distinct functional programs in response to different stimuli[68,69]. Advances in the field of immunometabolism have established that metabolic regulation shapes immune cells responses and the activation of immune cells requires metabolic reprogramming to fulfill cellular needs and exert their

effector functions[70]. Therefore, understanding immune cell metabolism is essential to use metabolism as a possible therapeutic target in diseases such as cancer.

Macrophages are leukocytes that participate in inflammation and tissue homeostasis. Macrophages typically derive from blood-circulating monocytes[71] and can be classified into two major groups – the "classically activated" M1 macrophages and the "alternatively activated" M2 macrophages (Figure 6). This classification was first proposed in 2000 by Mills[72], however, the M1/M2 paradigm is nowadays considered an oversimplification, because it only represents two extremes in a spectrum of possible macrophage activation states, as macrophages are able to adapt their phenotype depending on environmental cues[70,73,74]. Hence, the new proposed nomenclature to distinguish macrophage populations is "M1-like" macrophages and "M2-like" macrophages[75].

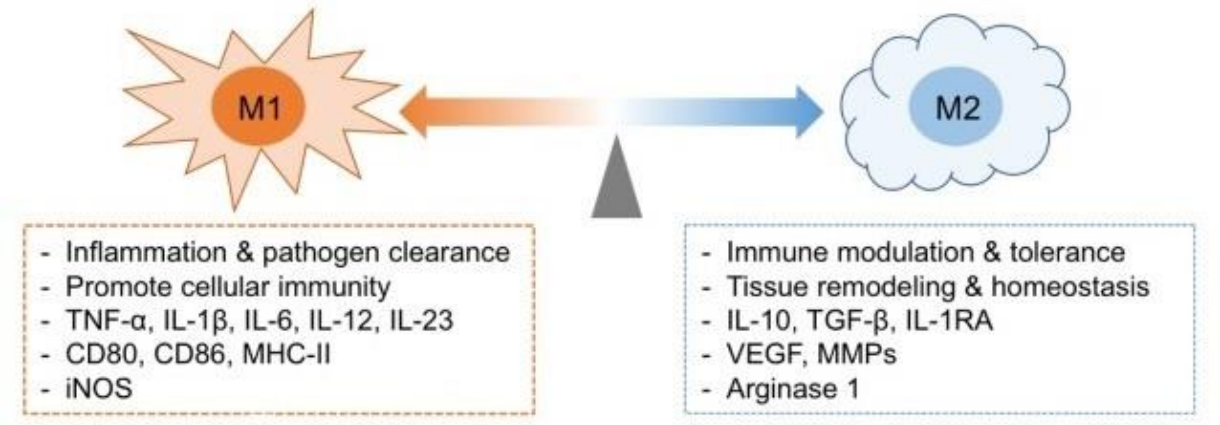


**Figure 6. Functional plasticity of macrophages.** Macrophages can be classified into classically activated (M1) or alternatively activated macrophages (M2). M1 macrophages produce pro-inflammatory cytokines and are responsible for driving inflammation while M2 macrophages produce anti-inflammatory cytokines and are linked to resolving inflammation and tissue remodeling. TNF-α: tumor necrosis factor alpha; MHC-II: major histocompatibility complex II; iNOS: inducible nitric oxide synthase; TGF-β: transforming growth factor beta; VEGF: vascular endothelial growth factor; MMPs: matrix metalloproteinases. Adapted from Thapa and Lee, 2019[81].

Macrophages upon stimulation with lipopolysaccharides (LPS), interferon-gamma (IFN-γ), and/or granulocyte-macrophage colony-stimulating factor (GM-CSF), are polarized towards an M1-like pro-inflammatory phenotype and produce pro-inflammatory cytokines including interleukin-1β (IL-1β), IL-12, IL-6, IL-18 and tumor necrosis factor-alpha (TNF-α). Besides pro-inflammatory cytokines, M1-like macrophages also produce reactive oxygen (ROS) and nitrogen species and have the ability to present antigens to T cells. M1-like macrophages are responsible for the clearance of pathogens and immune responses against neoplastic growth, thus they play an anti-tumorigenic role[75,76]. The metabolism of M1-like macrophages is characterized by enhanced aerobic glycolysis with the conversion of pyruvate into lactate, increased flux through the PPP, fatty acid synthesis and an impaired TCA cycle at the level of isocitrate dehydrogenase (IDH) and succinate dehydrogenase (SDH), leading to the accumulation of

citrate and succinate (Figure 7)[70]. The accumulation of citrate leads to the production of nitric oxide (NO), fatty acids and itaconate, an inhibitor of SDH[77]. Succinate accumulation stabilizes HIF-1α, inducing the expression of IL-1β and glycolytic genes[78,79]. Overexpression of the glucose transporter GLUT1 induces an M1-like phenotype, emphasizing the importance of glucose availability for the polarization of macrophages towards a pro-inflammatory phenotype[80]. Since the TCA cycle is impaired, lactate production regenerates the NAD+ needed to sustain glycolysis[81]. Enhanced PPP converts glycolytic intermediates to precursors of amino acids and nucleotides and generates nicotinamide adenine dinucleotide phosphate (NADPH), a co-factor required for inducible nitric oxide synthase (iNOS) to convert arginine into NO and citrulline[82]. NO inhibits mitochondrial respiration by modifying the electron transport chain (ETC)[83], and recent evidence demonstrated that inhibition of iNOS improved the mitochondrial function of M1-like macrophages and promoted repolarization of M1 into M2-like macrophages[84]. Furthermore, NADPH is essential to prevent cell damage by ROS[85]. The metabolic programming of M1-like macrophages contributes to their pro-inflammatory phenotype, underlining the link between macrophage metabolism and functionality.

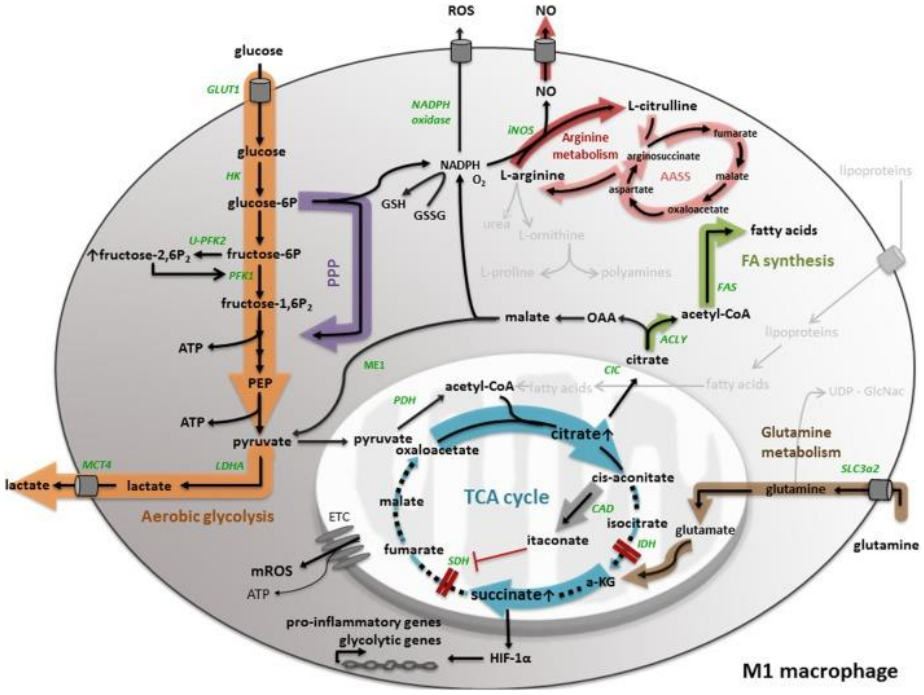


**Figure 7. M1-like macrophage metabolism.** M1 macrophage metabolism is characterized by enhanced aerobic glycolysis, with the conversion of pyruvate into lactate, increased flux through the PPP, fatty acid synthesis and an impaired TCA cycle, leading to the accumulation of citrate and succinate. Important metabolic pathways in M1-like macrophages are highlighted by the width of the colored shadow. Dotted lines represent impaired metabolic pathways. α-KG: α-ketoglutarate; AASS: aspartate–arginosuccinate shunt pathway; ACLY: ATP-citrate lyase; CAD: cis-aconitate decarboxylase; CIC: mitochondrial citrate carrier; ETC: electron transport chain; FAS: fatty acid synthase; GLUT1: glucose transporter 1; HK: hexokinase; IDH: isocitrate dehydrogenase; iNOS: inducible nitric oxide synthase; LDHA: lactate dehydrogenase A; MCT4: monocarboxylate transporter 4; ME: malic enzyme; OAA: oxaloacetate; PEP: phosphoenolpyruvate; PDH: pyruvate dehydrogenase; PFK: phosphofructokinase; SDH: succinate dehydrogenase; SLC: solute carrier. Image acquired from Geeraerts, et al., 2017[70].

Macrophages upon stimulation with IL-4, IL-10 and/or IL-13, are polarized towards an M2-like anti-inflammatory phenotype and produce anti-inflammatory cytokines including IL-10, transforming growth factor beta (TGF-β) and interleukin-1 receptor antagonist (IL-1RA). M2-like macrophages promote tissue remodeling, repair and immune tolerance, playing a pro-tumorigenic role[75,76]. The metabolism of M2-like macrophages is characterized by OXPHOS, fatty acid oxidation (FAO), decreased glycolysis and limited flux through the PPP[86]. While M1-like macrophages obtain their energy through glycolysis, M2-like macrophages produce ATP through an oxidative TCA cycle coupled to OXPHOS, and to fuel the cycle, they rely on FAO and glutamine metabolism (Figure 8)[87,88].

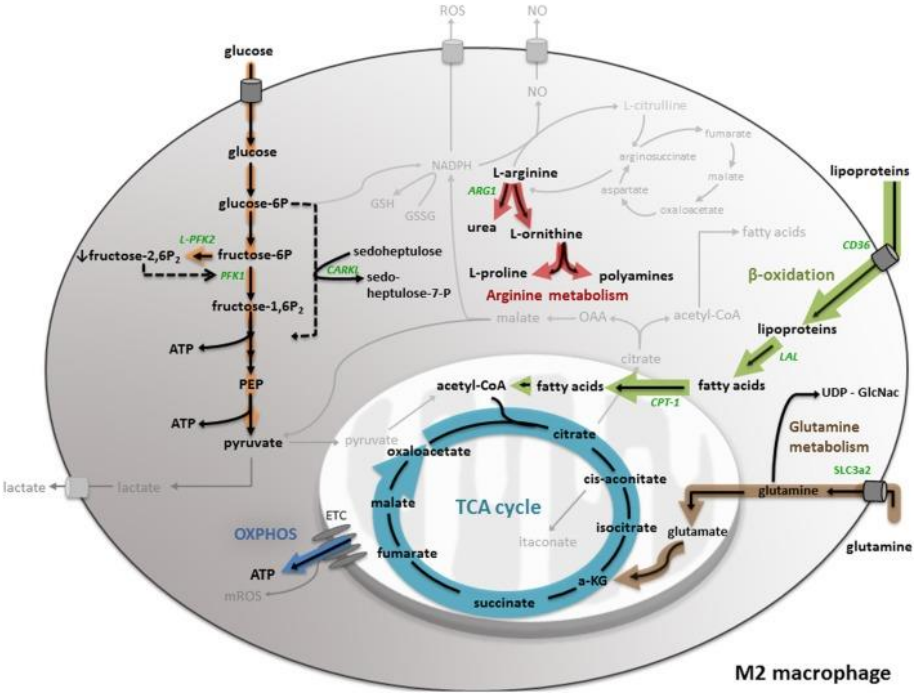


**Figure 8. M2-like macrophage metabolism.** M2-like macrophages metabolism is characterized by an oxidative TCA cycle coupled to oxidative phosphorylation (OXPHOS) to produce ATP. To fuel the cycle, M2-like macrophages rely on fatty acid oxidation and glutamine metabolism. Moreover, M2-like macrophages display a lowered glycolysis and pentose phosphate pathway. Important metabolic pathways in M2-like macrophages are highlighted by the width of the colored shadow. Dotted lines represent impaired metabolic pathways. α-KG: α-ketoglutarate; ARG1: arginase; CD36: cluster of differentiation 36; CPT: carnitine palmitoyl transferase; ETC: electron transport chain; LAL: lysosomal acid lipase; PEP: phosphoenolpyruvate; PFK: phosphofructokinase; SLC: solute carrier. Image acquired from Geeraerts, et al., 2017[70].

Besides the energy metabolism, M1-like and M2-like macrophages also display differences in the arginine metabolism. While M1-like macrophages convert arginine into NO and citrulline by iNOS, M2-like macrophages catalyze arginine to urea and ornithine by arginase (ARG-1), promoting wound repair[70]. In M2-like macrophages there is no production of NO, therefore the ETC is no longer impaired and enables ATP production through OXPHOS[84]. Glutamine can be used for the synthesis of amino acids and nucleotides and supply the TCA cycle in situations of impaired mitochondrial pyruvate transport[81,89]. Although glutamine metabolism is also associated with NO production, since glutamine can be converted

into arginine[90], recent evidence suggests that glutamine synthetase (GS) is upregulated in M2-like macrophages and modulates macrophages polarization towards an M2-like phenotype. Furthermore, inhibition of GS induced the expression of pro-inflammatory cytokines and enzymes, indicating the importance of glutamine metabolism on macrophage polarization[91].

The presence of TAMs at the tumor site is often associated with a poor clinical outcome, however, there is conflicting data in some types of cancer, such as stomach, prostate or lung cancer, in which both positive and negative associations have been reported[92]. Studies demonstrate that the majority of TAMs display M2-like properties and contribute to tumor progression by promoting angiogenesis, metastasis and immunosuppression (reviewed in [93]). M2-like TAMs release angiogenic growth factors such as vascular endothelial growth factor (VEGF)[94] and produce matrix metalloproteinases (MMPs) that degrade the basement membrane and help cancer cells EMT, promoting invasion and metastasis[95]. Furthermore, M2-like TAMs negatively regulates effector T cells and natural killer (NK) cells by the production of anti-inflammatory cytokines[96,97], while attracting immunosuppressive cells such as Treg cells and MDSCs[98,99]. Interestingly, the co-existence of two TAM subpopulations in the tumor tissue has already been described, with M1-like TAMs present in normoxic regions of the tumor while M2-like TAMs reside in the hypoxic regions of the tumor[100]. Casazza and co-workers demonstrated that depletion of neuropilin-1, a receptor for VEGF, prevented the migration of TAMs into the hypoxic regions of the tumor, leading to the accumulation of TAMs in the normoxic areas and reprogramming towards an M1-like phenotype, inhibiting tumor growth and metastasis[101]. A recent study also showed that hypoxia-induced tumor exosomes promote M2-like macrophage polarization[102].

Since the metabolism of macrophages is intrinsically connected to their functionality, metabolic reprogramming of M2-like TAMs started to gain attention as a potential way to repolarize TAMs towards an anti-tumoral phenotype. Recently, it was revealed a link between TAMs metabolism and tumor vasculature. Increased expression of regulated in development and DNA damage response 1 (REDD1), a negative regulator of mammalian target of rapamycin (mTOR), was observed in hypoxic TAMs and deletion of REDD1 induced mTOR activity, leading to upregulation of glycolysis. Enhanced glycolysis caused glucose competition between TAMs and tumor endothelial cells and as a result, tumor vasculature was stabilized, preventing angiogenesis and metastasis[103]. The metabolic interplay between cancer cells and TAMs in the TME raised questions about the impact of lactate on the metabolism of macrophages and to date, several studies demonstrate the effect of lactate on monocytes and macrophages *in vitro*. High levels of lactate (20 mM) at a pH of 7.4 inhibited monocyte migration in the Boyden chamber system[47]. Moreover, when cultured in the presence of lactate, monocytes and macrophages produce less pro-

inflammatory cytokines and chemokines and decrease their glycolytic rates[36,47,53]. After activation, both monocytes and macrophages rely on glycolysis to support their function[36,53]. In order to sustain glycolysis, lactate should be exported, however, extracellular acidification reduces the export of lactate by monocytes and macrophages, impairing glycolysis and consequently the expression of pro-inflammatory mediators[36,56]. Lactate can also have a signaling role in driving cancer immune evasion, as it was shown to induce M2-like macrophage polarization by activating the ERK/STAT3 signaling pathway in breast cancer[104], although others have proposed that high levels of tumor-derived lactate drives M2-like macrophage polarization through stabilization of HIF-1α, increasing the levels of arginase and VEGF[105,106]. Interestingly, an acidic pH was unable to stabilize HIF-1α, and lactate needed the presence of protons to exert its effect, suggesting that acidification of the medium synergizes with lactate to promote an immunosuppressive environment. GPR132 (G protein coupled-receptor 132), a lactate receptor/sensor highly expressed in macrophages, promotes the M2-like phenotype, facilitating breast cancer metastasis[107]. Furthermore, lactate derived from a pancreatic tumour cell line induced polarization of THP-1, a human monocytic cell line, into an M2-like phenotype[108] and in a microfluidic device, lactate exported by bladder cancer cells reprogrammed TAMs to an M2-like phenotype[109]. A recent study explored the relationship between lactate concentration and pro-tumoral (M2) macrophage polarization in biopsies from patients with head and neck squamous cell carcinoma (HNSCC), by measuring the expression of colony stimulating factor 1 receptor (CSF1R) and CD163, both M2 macrophage markers. Tumors with high lactic acid concentration showed higher levels of CSF1R and CD163 expression, suggesting that tumor-derived lactate promotes M2-like macrophage polarization in human HNSCC[110]. In summary, this data show that tumor-derived lactate skews macrophages towards a pro-tumoral phenotype.

## 1.4 Monocarboxylate transporters

Monocarboxylate transporters (MCTs) are a family of transporter proteins composed by 14 members and is encoded by the *Solute Carrier 16* (*SLC16*) gene family[111]. Among MCTs, the first four isoforms, *slc16a1*/MCT1, *slc16a7*/MCT2, *slc16a8*/MCT3 and *slc16a3*/MCT4, are the most widely understood and known to mediate the proton-linked plasma membrane transport of monocarboxylates molecules such as lactate, pyruvate and ketone bodies, being lactate the primary substrate[112].

MCTs have different substrate affinities and can direct both the influx and efflux of lactate across biological membranes. In this regard, MCT1 is ubiquitously expressed in almost all tissues, has intermediate affinity for lactate ($K_m \approx 3mM$) and can uptake or release lactate and other monocarboxylates

through the plasma membrane, according to cellular metabolic needs. MCT2 has the highest affinity for lactate ($K_m \approx$ 1mM), is responsible for the uptake of lactate and is poorly expressed in human tissues, however, in mouse, rat and hamster, MCT2 is primarily expressed in the liver, kidney and brain, facilitating the uptake of lactate as an alternative metabolic fuel. MCT3 expression is restricted to the retinal pigment epithelium and choroid plexus epithelia, where it mediates the efflux of lactate out of the retina. MCT4 displays the lowest affinity for lactate ($K_m \approx$ 30mM) and is mostly expressed in high glycolytic tissues and cells such as skeletal muscle fibers, astrocytes and leukocytes, being responsible for the export of lactate[111]. Ancillary proteins are required for the functional expression of MCTs, as they are involved in trafficking and anchoring of MCTs at the plasma membrane. MCT1, MCT3 and MCT4 are associated with the chaperone protein basigin (also known as cluster of differentiation 147, CD147), while MCT2 is associated with the protein embigin[113]. Of note, the transport of lactate relies on the extracellular versus intracellular concentration of lactate, the pH and the concentration of other substrates of MCTs[114].

As already stated, cancer cells export lactate to sustain their typical glycolytic metabolism. The transport of lactate is mainly mediated by MCT1 and/or MCT4 isoforms, in order to maintain the glycolytic rate of cancer cells[50]. MCT4 is upregulated by HIF-1α and proton-linked export of lactate avoids glycolysis inhibition due to a negative feedback mechanism and plays an important role in the regulation of intracellular pH, avoiding lactic acidosis[48,115,116]. MCT1 is regulated by the tumor suppressor gene *p53*, in which *p53*-deficient tumors display higher expression of MCT1, allowing cancer cells to adapt to metabolic needs by importing or exporting lactate depending on glucose availability[117]. The distribution pattern of these two MCTs is different between tumor types, due to disparities in lactate content and the oncogenic pathways that drive each cancer[65]. Several types of human cancer, such as breast, lung, prostate, colon, stomach and glioblastoma show increased expression of MCT1 and MCT4, which has been associated with a poor prognosis (reviewed in [118]).

### 1.4.1 The role of MCTs in lactate shuttles

Once thought to be a metabolic waste product, it is now known that lactate can be used as a major energy source and a signaling molecule. As the end product of one metabolic pathway (glycolysis) and the substrate for another metabolic pathway (mitochondrial respiration), the lactate shuttle hypothesis depicts lactate as the link between glycolytic and oxidative pathways[119].

This lactate shuttle mechanism has already been described between working skeletal muscles and the heart and also between astrocytes and neurons[120,121]. During exercise, glycolytic muscle fibers

produce lactate and release it through MCT4[122]. Lactate is then transported into red blood cells via MCT1 and the heart uptakes lactate from the blood through MCT1 and oxidizes it to fuel its functions[120,123]. Similarly, Magistretti and Pellerin reported that astrocytes display a high glycolytic metabolism and export lactate via MCT4, while neurons import lactate via MCT2 and use it as an energy substrate for oxidative-derived ATP production[121].

Established tumors consist of different types of cancer cells and possess regions adjacent to blood vessels where oxygen availability is enough and regions with low tension of oxygen, or hypoxic regions. The discovery of expression of MCT1 in well-oxygenated regions of the tumor and MCT4 in hypoxic regions of the tumor, suggested a metabolic symbiosis between cancer cells within a tumor[124,125]. This symbiosis is based on a lactate shuttle, in which hypoxic cancer cells rely on glycolysis to produce ATP and export lactate through MCT4, while oxygenated cancer cells import lactate via MCT1 and lactate is oxidized to fuel the TCA cycle for ATP production (Figure 9)[124]. This metabolic cooperation allows the glucose supply to be preferentially consumed by hypoxic cancer cells.

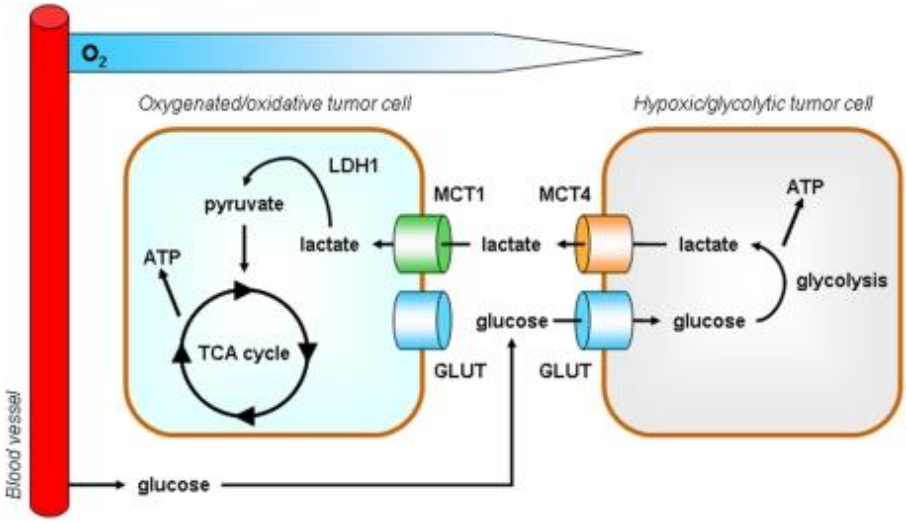


**Figure 9. Lactate shuttle between glycolytic and oxidative cancer cells**. Glycolytic cancer cells in hypoxic regions export lactate through MCT4, while oxidative cancer cells in oxygenated regions uptake lactate to support ATP production. Image acquired from Porporato et al., 2011[16].

Besides the role in metabolic cooperation between hypoxic and oxygenated cancer cells, lactate is also involved in the crosstalk between cancer cells and endothelial, stromal and immune cells[126]. In the vascular endothelial lactate shuttle, cancer cells export lactate via MCT4 which endothelial cells uptake via MCT1 (Figure 10). Rather than a metabolic substrate, lactate functions as a signaling molecule, as lactate uptake and conversion to pyruvate stabilizes HIF-1α and activates the autocrine NF-kB/IL-8 pathway, inducing endothelial cell migration, tube formation and tumor angiogenesis[127].

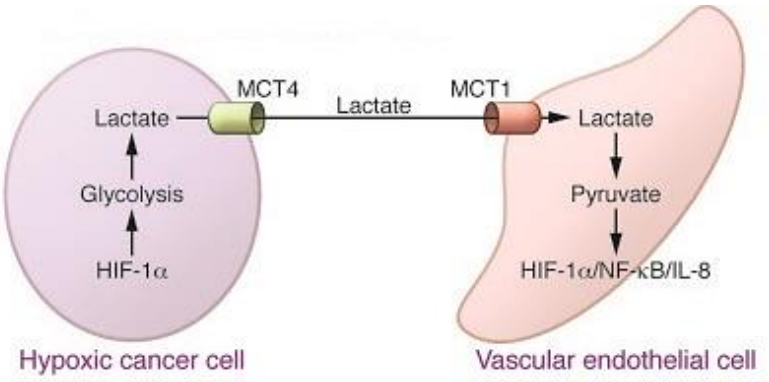


**Figure 10. Lactate shuttle between cancer cells and endothelial cells.** Cancer cells efflux lactate via MCT4, which is imported by vascular endothelial cells via MCT1, promoting endothelial cell migration, tube formation and tumor angiogenesis. Adapted from Doherty and Cleveland, 2013[136].

Cancer-associated fibroblasts (CAFs) are one of the most abundant stromal cell type in the tumor microenvironment[128]. Pavlides et al. proposed a lactate shuttle involving MCTs between CAFs and cancer cells. In this process, oxidative cancer cells induce an oxidative stress in CAFs by secreting ROS, such as hydrogen peroxide, which will activate HIF-1α, glycolysis and consequently, lactate export via MCT4 by the CAFs. Lactate is then imported via MCT1 and used oxidatively by cancer cells to support ATP production (Figure 11)[129]. *In vitro,* co-culture of breast cancer cells with fibroblasts upregulated MCT4 expression in the fibroblasts and MCT1 expression in cancer cells[130].

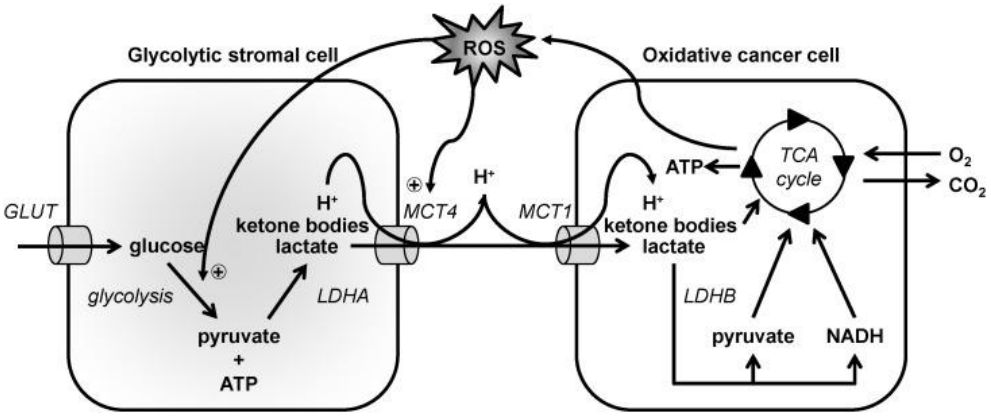


**Figure 11. Lactate shuttle between oxidative cancer cells and stromal cells in the tumor microenvironment**. Oxidative cancer cells produce reactive oxygen species (ROS) such as hydrogen peroxide that induce an oxidative stress in stromal cells, promoting glycolysis and export of lactate via MCT4. Oxidative cancer cells import lactate via MCT1, and lactate is oxidized to pyruvate to fuel the TCA cycle for production of ATP. Image acquired from Escuredo et al., 2016[126].

Since the TME is very heterogeneous, cancer cells and immune cells face competition to obtain nutrients such as glucose, fatty acids, amino acids and metabolites such as lactate[131]. Highly glycolytic malignant cells, besides restricting immune cells metabolically and therefore interfere with their function, also release immunosuppressive metabolites such as lactate, forming a metabolic interplay with immune cells (Figure 12)[132,133]. It is thought that cancer cells use shuttling of metabolites as a route to evade the immune system. On one hand, high concentrations of lactate exported by cancer cells via MCT1/4, coupled with metabolic competition between cancer and immune cells, disturbs immune cells metabolism and function, creating a metabolic antagonism; on the other hand, oxidative immune cells import lactate via MCT1/2 and oxidize it as an energy source, or act as a signaling molecule, providing them with an advantage in high-lactate conditions, creating a metabolic symbiosis[133].

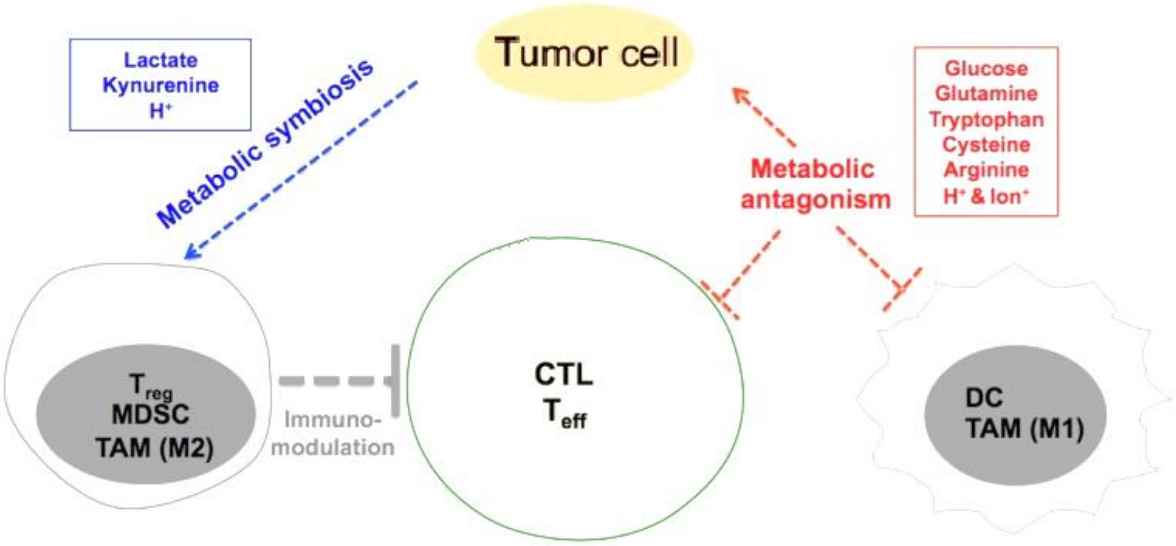


**Figure 12. Shuttling of metabolites between cancer cells and immune cells.** Cancer cells establish a metabolic interplay with immune cells through shuttling of metabolites. Dendritic cells (DC), tumor-associated macrophages M1 (TAM-M1), cytoxic T cells (CTL) and T effector cells (Teff) form a metabolic antagonism with cancer cells, while regulatory T cells (Treg), myeloid-derived suppressor cells (MDSC) and tumor-associated macrophages M2 (TAM-M2) utilize metabolites from cancer cells, forming a metabolic symbiosis. Adapted from Wang, et al., 2014[133].

### 1.4.2 MCTs as therapeutic targets

Given the importance of lactate to tumorigenesis, targeting lactate production and transport has been proposed as a therapeutic strategy, with MCTs as potential targets for cancer therapy.

There is evidence that knockdown of MCT4 impairs breast cancer cells ability to migrate and the accumulation of intracellular lactate leads to cancer cell death[134,135]. Furthermore, inhibition of MCT1 reduces cancer cell proliferation[124,136,137]. The anticancer drug lonidamine has been reported to decrease the intracellular pH of neuroblastoma cell lines due to unspecific inhibition of MCTs[138]. The use of

quercetin, a flavonoid that inhibits MCTs, disrupted the lactate shuttle between bladder cancer cells and TAMs in a microfluidic device[109]. The small molecule α-cyano-4-hydroxy-cinnamate (CHC), a classical MCT inhibitor, has been used in preclinical models due to its ability to induce apoptosis and impairing cell proliferation and migration[139]. In fact, our team has already described the effects of CHC and quercetin in a panel of different breast cancer cell lines. Glycolytic breast cancer cell lines expressing MCT1, upon exposure to lactate transport inhibitors, suffered a decrease in glucose consumption, lactate production and total biomass. However, the cell line MDA-MB-231, negative for MCT1 expression, was the most sensitive to both CHC and quercetin, indicating that the effect of these inhibitors on this cell line may be due to other mechanisms, besides blocking the transport of lactate[140]. Although these compounds present anti-cancer effects, they lack MCT specificity[141]. Recently, a new class of highly specific inhibitors for MCTs was developed by AstraZeneca. AR-C155858 was the first-generation of a highly selective and potent inhibitor for MCT1/2, with a binding affinity for MCT1 of 2.3nM, and demonstrated inhibition of MCT1 in breast cancer cells and transformed fibroblasts[142,143]. Furthermore, AZD3965, a second-generation MCT1 inhibitor with activity against MCT2, derived from AR-C155858, displays a binding affinity for MCT1 of 1.6nM[144]. AZD3965 demonstrated its effects by disrupting lactate efflux and reducing tumor growth *in vitro* as well as *in vivo*[145,146]. In addition, AZD3965 has good oral bioavailability and is currently undergoing phase I/II clinical trials for patients with solid tumors[147].

The functional redundancy between MCT1 and MCT4 enables tumors to be insensitive to inhibition of one isoform, due to a compensation mechanism with the other isoform. It has already been described that MCT1 inhibition led to an increase in MCT4 expression[145] and this rendered cancer cells insensitive to MCT1 inhibition, resulting in tumor growth[148]. Additionally, knockdown of MCT4 made cancer cells sensitive to MCT1 inhibition, leading to a decrease in tumor growth[148]. Considering that most of highly aggressive tumors express MCT4[118], there was a need for specific MCT4 inhibitors. AstraZeneca developed a specific and effective inhibitor for MCT4, AZ93, which in combination with AZD3965 abolishes colon adenocarcinoma cells growth, however solo inhibition of MCT4 by AZ93 did not impact cell growth[149].

Based on the evidence that tumor-derived lactate creates an immunosuppressive TME by modulating immune cell function, and the key role that MCTs play in this metabolic interplay, we hypothesized that disrupting the release of lactate from tumor cells or the import of lactate by immune cells, through MCTs, will revert the pro-tumoral phenotype displayed by immune cells, namely TAMs.

# CHAPTER 2 | OBJECTIVES

Increasing evidence indicates that tumor-derived lactate creates an immunosuppressive microenvironment by modulating immune cell function. In fact, the immunosuppressive role of lactate has been shown to modulate tumor associated macrophages towards a pro-tumoral phenotype, supporting tumor growth. Due to the importance of MCTs on the transport of lactate, we hypothesized that disrupting this metabolic interplay between cancer cells and tumor associated macrophages, by targeting MCTs, could reprogram macrophages towards an anti-tumoral phenotype. For that purpose, the objectives of this master thesis were:

I. Characterize the expression of MCTs on cancer cells and tumor associated macrophages in a murine tumor model;

II. Generate and characterize the metabolic profile of MCT1 and MCT4 knockout cancer cells;

III. Dissecting the role of MCT knockout on the polarization of tumor associated macrophages.

# CHAPTER 3 | MATERIALS AND METHODS

## 3.1 Cell lines and cell culture

The murine Lewis lung carcinoma cell line LLC1 and the murine medullary breast adenocarcinoma cancer cell line E0771 were used in this study. The LLC1 cell line was established from the Lewis lung carcinoma, a spontaneous carcinoma of the lung of a C57BL mouse discovered by Dr. Margaret R. Lewis[150]. This cell line displays both adherent and suspension cell populations, can take a couple of days until cells grow as an adherent monolayer and has a doubling time of 21 hours. The E0771 cell line was isolated from a spontaneous tumor from C57BL/6 mouse and adapted for anti-cancer drug testing[151]. E0771 cells grow as an adherent monolayer. LLC1 cell line was obtained from American Type Culture Collection (ATCC® CRL-1642™) and E0771 cell line from European Collection of Authenticated Cell Cultures (ECACC). Both cell lines were maintained in Dulbecco's Modified Eagle Medium (DMEM) (Biochrom®), supplemented with 10% of fetal bovine serum (FBS) (Biochrom®) and 1% of antibiotic Penicillin-Streptomycin (Pen-Strep) (Gibco®) and incubated in a humidified atmosphere of 21% $O_2$, 5% $CO_2$ and 74% $N_2$ at 37°C. FBS contains growth factors, enzymes and other chemical components required for sustained cell growth[152] and Pen-Step is an antibiotic used to maintain sterile conditions and prevent bacterial contaminations[153].

## 3.2 Immunohistochemistry

Immunohistochemistry analysis was used to evaluate the expression of CD68 on paraffin-embedded tissue sections from LLC1 subcutaneous tumors in C57BL/6 mice. Immunohistochemistry was performed based on the streptavidin-biotin-peroxidase complex principle with the Ultravision Detection System Anti-polyvalent, HRP (Lab Vision Corporation, Thermo Scientific™). In brief, paraffin embedded sections were deparaffinized in xylene and hydrated in a graded series of ethanol solutions. For antigen retrieval, sections were incubated with citrate buffer (pH 6.0) for 20 minutes in a water bath at 98°C, followed by 20 minutes at room temperature. Endogenous peroxidases were inactivated by incubating sections with 3% hydrogen peroxide in methanol for 10 minutes at room temperature. Tissue sections were incubated with blocking solution for 10 minutes and incubated with primary antibody CD68 (mouse sc-20060, Santa Cruz Biotechnology®) for 2 hours at room temperature. Sections were then incubated with biotinylated goat anti-polyvalent secondary antibody for 10 minutes and streptavidin peroxidase for 10 minutes. To visualize the reaction, tissues were stained with 3,3′-Diamonobenzidine

(DAB Quanto Chromogen, Thermo Scientific™) as a chromogen for 10 minutes, counterstained with haematoxylin and mounted.

## 3.3 Immunofluorescence

Immunofluorescence analysis was used to evaluate the expression of CD68, MCT1, MCT2 and MCT4 on paraffin-embedded tissue sections from LLC1 subcutaneous tumors in C57BL/6 mice. In brief, paraffin embedded sections were deparaffinized in xylene and hydrated in a graded series of ethanol solutions. For antigen retrieval, sections were incubated with citrate buffer (pH 6.0) for 20 minutes in a water bath at 98°C, followed by 20 minutes at room temperature. Tissue sections were then incubated in 5% bovine serum albumin (BSA) for 30 minutes to block non-specific secondary antibody binding. Next, incubation with primary antibodies diluted in 5% BSA was performed overnight at room temperature (Table 1). In the following day, tissue sections were incubated with secondary antibodies for 1 hour at room temperature (Table 2). Tissue sections were mounted using Fluoroshield Mounting Media containing 4′,6-diamidino-2-phenylindole (DAPI, Sigma-Aldrich). Images were obtained with an Olympus BX61 fluorescent microscope, using CellSens software.

**Table 1. Primary antibodies used in immunofluorescence analysis.**

| Protein | Reference | Dilution |
|---|---|---|
| CD68 | mouse SC-20060 (Santa Cruz Biotechnology®) | 1/300 |
| MCT1 | rabbit ab3538p (Merck Millipore) | 1/300 |
| MCT2 | rabbit SC-503222 (Santa Cruz Biotechnology®) | 1/100 |
| MCT4 | rabbit SC-50329 (Santa Cruz Biotechnology®) | 1/300 |

**Table 2. Secondary antibodies used in immunofluorescence analysis.**

| Protein | Reference | Dilution |
|---|---|---|
| Alexa Fluor 488 goat anti-rabbit | A11008 | 1/400 |
| Alexa Fluor 594 goat anti-mouse | A11302 | 1/200 |

## 3.4 Generation of MCT1 and MCT4-null cells

E0771 KO cells for MCT1 and MCT4 were generated using the Clustered Regularly Interspaced Short Palindromic Repeat (CRISPR) system. The CRISPR utilizes an RNA-guided endonuclease, Cas9, which is capable of making site-specific cuts at DNA sequences targeted specifically by a guiding RNA molecule[154]. For MCT1 KO, E0771 cells were co-transfected with a mouse MCT1 CRISPR/Cas9 KO Plasmid (SC-422976, Santa Cruz Biotechnology®) and a mouse MCT1 HDR Plasmid (SC-422976-HDR, Santa Cruz Biotechnology®), using JetPRIME® transfection reagent (Polyplus-transfection SA), according to manufacturer's instructions. For MCT4 KO, E0771 cells were co-transfected with a mouse MCT4 CRISPR/Cas9 KO Plasmid (SC-429828, Santa Cruz Biotechnology®) and a mouse MCT4 HDR Plasmid (SC-429828-HDR, Santa Cruz Biotechnology®), using JetPRIME® transfection reagent (Polyplus-transfection SA), according to manufacturer's instructions. The CRISPR/Cas9 technology induces a double stranded break (DSB) in the genome of cells and this DSB can be repaired by homology-directed repair (HDR), allowing for precise gene editing at the DSB site[154]. The CRISPR/Cas9 KO Plasmid incorporates a green fluorescent protein (GFP) gene, while the MCT1 and MCT4 HDR Plasmid incorporates a red fluorescent protein (RFP) gene and a puromycin resistance gene, therefore we were able to enrich the pool of successfully transfected cells by addition of puromycin, and sort for MCT1 and MCT4-null cells based on the double expression of RFP/GFP by fluorescence-activated cell sorting (FACS). The absence of MCT1/4 expression was confirmed by Western blot.

## 3.5 Western Blot

Western blot analysis was used to validate the knockout of MCT1 and MCT4 by the CRISP/Cas9 technique in E0771 cells and the transfection of small interfering RNA (siRNA) targeting MCT2 in bone marrow-derived macrophages (BMDM). E0771 WT, E0771 C1.51 and E0771 C4.14 cells were grown to 80% confluency. BMDM were collected for protein extraction 72 hours after transfection with siRNA. BMDM were washed in PBS at room temperature while the rest of the cells were washed in cold phosphate-buffered saline (PBS), lysed and scraped in lysis buffer (50mM Tris pH 7.6-8.0; 150mM NaCl; 5mM EDTA; 1mM Na3VO4; 10mM NaF; 10mM Na4P2O7; 1% Triton X-100) supplemented with proteases inhibitors (Roche®), homogenized for 15 minutes, and then centrifuged at 13000rpm for 15 minutes at 4°C. Total protein quantification was performed using the colorimetric Bradford method, in which the binding of proteins to the Coomassie Blue dye results in a color change from brown to blue[155]. 30µg of protein were added to an equal volume of Laemmli loading buffer 2x (Bio-Rad) and denatured for 5

minutes at 98°C in the Thermoblock. Proteins were loaded and ran in a 10% sodium dodecyl sulfate–polyacrylamide gel electrophoresis (SDS-PAGE), that allows protein separation by mass. The polyacrylamide gels were transferred for 30 minutes, using the Trans-Blot Turbo transfer system (Bio-Rad), onto a nitrocellulose membrane (Amershan Biosciences). Membranes were blocked in 5% skim milk in TBS 1x 0.1% Tween 20 buffer for 1 hour and incubated overnight with the primary antibodies at 4°C (Table 3). In the following day, membranes were washed with TBS 1x 0.1% Tween 20 and incubated with the secondary antibodies coupled to horseradish peroxidase (HRP), for 1 hour at room temperature (Table 4). Proteins levels were detected by chemiluminescence after incubation with Supersignal™ West Fento Maximum Sensitivity Substrate (Thermo Scientific™) using the ChemiDoc™ XRS System (Bio-Rad).

**Table 3. Primary antibodies used in Western blot.**

| Protein | Reference | Dilution |
|---|---|---|
| MCT1 | mouse SC-365501 (Santa Cruz Biotechnology®) | 1/500 |
| MCT2 | goat SC-14926 (Santa Cruz Biotechnology®) | 1/500 |
| MCT4 | mouse SC-376465 (Santa Cruz Biotechnology®) | 1/400 |
| Tubulin | mouse BL605102 (BioLegend®) | 1/1000 |

**Table 4. Secondary antibodies used in Western blot.**

| Protein | Reference | Dilution |
|---|---|---|
| Goat anti-mouse IgG-HRP | SC-2031 (Santa Cruz Biotechnology®) | 1/5000 |
| Donkey Anti-goat IgG-HRP | SC-2020 (Santa Cruz Biotechnology®) | 1/3000 |

## 3.6 Cell biomass analysis

The effect of MCT knockout on total cell biomass was measured by the Sulforhodamine B (SRB, Sigma-Aldrich) assay. E0771 WT, E0771 C1.51 and E0771 C4.14 cells were seeded $3x10^3$ cells per well in 96-well plates and allowed to adhere overnight. E0771 C1.51 and parental cells were incubated in standard DMEM medium (high glucose, 25mM) or in DMEM low glucose (5mM) with 50μM of phenformin. E0771 C4.14 and parental cells were incubated in DMEM with 50μM of phenformin and

300nM of the MCT1 inhibitor AZD3965 alone, or a combination of both. After 24 hours, 48 hours and 72 hours, cells were fixed with cold 10% trichloroacetic acid (TCA) for 1 hour at 4°C. Then, cells were stained with SRB for 30 minutes. SRB is a dye that binds to the protein content of cells and colorimetric evaluation of the amount of dye in stained cells provides an estimation of total protein mass, which is proportional to cell number[156]. The excess of dye was removed by washing cells with 1% acetic acid and then air dry the plate at room temperature. Protein-bound dye was dissolved by adding 10mM Tris-Base solution to each well and shake the plate on an orbital shaker for about 10 minutes. The absorbance was measured at 530nm in the plate reader Thermo Scientific Varioskan® Flash.

## 3.7 Glucose and lactate measurement

The metabolic behavior of the cell lines under the different treatments was determined by analyzing the extracellular amounts of glucose and lactate. E0771 WT, E0771 C1.51 and E0771 C4.14 cells were seeded $5x10^4$ cells per well in 48-well plates and allowed to adhere overnight. E0771 C1.51 and WT cells were incubated in standard or low glucose DMEM with 50μM of phenformin. E0771 C4.14 and WT cells were incubated in DMEM with 50μM of phenformin and 300nM of the MCT1 inhibitor AZD3965 alone, or a combination of both. After 24 hours, glucose and lactate content were analyzed in the cell culture supernatant using a commercial kit (Spinreact®), in which 100μl of the commercial reagent is added to 2μl of the sample for 10 minutes in 96-well plates. After 10 minutes, glucose and lactate were quantified by the Thermo Scientific Varioskan® Flash readout at 490nm for lactate and 505nm for glucose. The results were normalized against total biomass (μg/total biomass), which was assessed through SRB assay, as reported above.

## 3.8 Bone marrow-derived macrophages isolation

For the isolation of bone marrow-derived macrophages (BMDM), 8 weeks old C57BL/6 mice were euthanized by cervical dislocation. With the help of a surgical scissor and tweezers, the tibia and femur were dissected and the skin around the legs and the muscle around the bones removed with the help of sterile gauze. The bones were then placed on cold PBS on ice. The tips of the bones were cut and then the bones were flushed with cold DMEM, using a 25G needle (Terumo®), into a Petri dish. The cellular suspension was collected with a 21G needle (Terumo®) and transferred to a 50ml Falcon tube passing through a 40μm filter (Falcon®). The cells were then centrifuged for 6 minutes at 1200 rpm at

4°C and counted by mixing 10μl of cell suspension with 10μl of Trypan Blue (Gibco®) on a Neubauer Chamber. $8x10^6$ bone marrow cells were seeded per 90mm Petri dish (Thermo Scientific™ Sterilin™) in complete Dulbecco's Modified Eagle's Medium (cDMEM), containing 10% FBS, 1% Pen-Strep, 1% Sodium Pyruvate (Gibco®), 1% Glutamine (Gibco®) and 1% 4-(2-hydroxyethyl)-1-piperazineethanesulfonic acid (HEPES, Gibco®) and supplemented with 30% of L929-cell conditioned medium (LCCM). Sodium Pyruvate is added as a carbon source in addition to glucose[157]. Glutamine provides nitrogen for the synthesis of proteins, nucleic acids and other nitrogenous compounds[158]. HEPES is a zwitterionic organic chemical buffering agent, used to maintain physiological pH[159]. LCCM is used as a source of macrophage colony-stimulating factor (M-CSF), a cytokine necessary for the differentiation of bone marrow cells into BMDM[160,161]. Cells were incubated in a humidified atmosphere of 21% $O_2$, 5% $CO_2$ and 74% $N_2$ at 37°C for up to 6 days. At day 3 of culture, 3ml of additional cDMEM medium supplemented with 30% LCCM were added to each Petri dish. At day 6 of culture, macrophages were harvested with 6ml of cold PBS per Petri dish and with the plunger of a syringe, cells were gently scrapped from the dish and placed in a Falcon tube. The cellular suspension was centrifuged for 5 minutes at 1200 rpm and the cell pellet was resuspended in cDMEM without the supplementation of LCCM. The number of cells was determined by mixing 10μl of the cellular suspension with 10μl of Trypan Blue (Gibco®) on a Neubauer Chamber. Then, approximately $2x10^6$ BMDM were seeded in 6-well plates in cDMEM and allowed to rest for 1-2 hours until further experiments were performed.

For the production of LCCM, $9,4x10^5$ cells of the murine fibroblasts cell line L929 were seeded in a T175 flask containing 110ml of DMEM supplemented with 10% FBS, 1% Pen-Strep and 1% HEPES and incubated in a humidified atmosphere of 21% $O_2$, 5% $CO_2$ and 74% $N_2$ at 37°C for 7 days. After 7 days, the medium is collected, centrifuged and filtrated and is stored at -20°C for further use.

## 3.9 Co-culture experiments

$5x10^5$ of LLC1, E0771 WT, E0771 C1.51 and E0771 C4.14 cells were seeded in 6-well transwell inserts (Millicell®, #MCHT06H48) the day before co-culture with BMDM. Afterwards, the transwell inserts were inserted in the 6-well plate well containing approximately $2x10^6$ BMDM and the medium of the well was changed to DMEM with 5mM of glucose, in an effort to resemble *in vivo* conditions, since glucose levels in solid tumors are known to be low[162]. The cells were then incubated in a humidified atmosphere of 21% $O_2$, 5% $CO_2$ and 74% $N_2$ at 37°C for 24 hours. After 24 hours, the medium was collected, filtered and stored for ELISA assays, while BMDM were harvested for RNA extraction.

## 3.10 RNA Extraction

RNA from bone marrow-derived macrophages was extracted using the TripleXtractor directRNA Kit (Grisp, #GK23.0100), according to manufacturers' instructions. The TripleXtractor directRNA combines the lysis ability of the phenol/guanidine thiocyanate solution "TripleXtractor Direct" with a spin column system for effective purification of RNA without the need for chloroform phase separation and isopropanol precipitation. The guanidine thiocyanate solution is a protein denaturant, used to lyse cells and to protect nucleic acids by preventing the activity of DNase and RNase enzymes [163]. Culture medium is removed and 1ml of TripleXtractor Direct was added to each well to promote cell disruption and, with the help of cell scrapers, the cellular suspension was recovered to an Eppendorf tube and then allowed to rest at room temperature for 5 minutes. The suspension was centrifuged for 1 minute at 16000g and the supernatant was transferred to a new RNase-free Eppendorf tube, to which was added absolute ethanol at a ratio 1:1 and mixed by vortex. An RNA binding column was placed in a collection tube and the mixture of cell suspension with absolute ethanol was passed through the RNA binding column and centrifuged for 1 minute at 16000g. The flow-through was discarded and the RNA binding column was washed three times with a wash buffer with three centrifugations for 30 seconds at 16000g. The flow-through was once again discarded and one centrifugation for 3 minutes at 16000g was performed to dry the matrix of the RNA binding column. The RNA binding column was transferred to a new RNase-free Eppendorf tube and 15 µl of RNase-free water were added to the center of the column and allowed to rest at room temperature for 1-2 minutes. Afterwards, one centrifugation for 1 minute at 16000g was performed to elute total RNA. RNA was then heated at 60°C for 5 minutes in a Thermoblock to promote its solubilization and stored at -20°C for short term storage or at -80°C for long term storage. RNA concentration was measured using the NanoDrop™ ND-1000 Spectrophotometer and the purity assessed through the A260/280 and A260/230 ratios.

## 3.11 Complementary DNA (cDNA) synthesis

Reverse transcription of RNA was carried out using Xpert cDNA Synthesis Mastermix kit (Grisp, #GK81.0100), according to manufacturer's instructions. In a RNase-free eppendorf tube, mix 10µl of Mastermix (2x), the volume correspondent to 1µg of RNA and then RNase-free water to make up to 19µl. Using a thermocycler (MyCycler Thermal Cycler, Bio-Rad), the sample was heated for 5 minutes at 65°C and then placed on ice for 2 minutes. Next, it was added 1µl of Xpert RTase (200U/µl) to the eppendorf

and mix thoroughly. The sample was placed in the thermocycler and incubated for 10 minutes at 25°C, followed by 15 minutes at 50°C and then 5 minutes at 85°C. The resultant cDNA was stored at -20°C.

## 3.12 Real-Time Quantitative Polymerase Chain Reaction (RT-qPCR)

RT-qPCR was used to assess the abundance of transcripts in a given sample[164]. Evaluation of M1-like and M2-like gene markers expression was performed using Xpert Fast Probe Mastermix (Grisp, #GE030.5100) and Taqman™ Probes, according to the volumes of Table 5, the amplification program illustrated in Table 6 and the Taqman™ Probes used are listed in Table 7. *HPRT* was used as the reference gene to calculate fold change in the expression of M1 and M2 genes. ΔCt values were first obtained: ΔCt= Threshold cycle (Ct) of *HPRT* - Ct of the gene. ΔΔCt values were then obtained: ΔΔCt=ΔCt of treated groups–ΔCt of untreated control groups. Fold change was calculated as 2-ΔΔCt, with control groups as 1- fold.

**Table 5. Volumes of RT-qPCR mixture used per each sample in evaluating M1 and M2 gene expression.**

| | |
|---|---|
| **Xpert Fast Probe Mastermix** | 5µl |
| **TaqMan Probe** | 0.5µl |
| **cDNA** | 1µl |
| **Nuclease-free water** | 3.5µl |
| **Total Volume** | **10µl** |

**Table 6. RT-qPCR amplification program using ABI Prism 7500 (Applied Biosystems).**

| Step | Temperature (°C) | Duration | Cycles |
|---|---|---|---|
| **Initial Denaturation and Enzyme Activation** | 95 | 10min | 1 |
| **Denaturation** | 95 | 15s | 40 |
| **Annealing** | 60 | 30s | |
| **Extension** | 72 | 30s | |

**Table 7. TaqMan™ probes used in RT-qPCR experiments.**

| Gene | Reference |
|---|---|
| *Ccl2* | Mm00441242_m1 |
| *Nos2* | Mm00440502_m1 |
| *Tnf* | Mm00443258_m1 |
| *Arg1* | Mm00475988_m1 |
| *Chi3l3* | Mm00657889_mH |
| *CD163* | Mm00474091_m1 |
| *Hprt* | Mm01545399_m1 |

For assessing MCTs expression, we used SYBR™ Green Mastermix (Applied Biosystems™), according to the volumes of Table 8, the amplification program illustrated in Table 9 and primers for *MCT1, MCT2, MCT4* and *TBP*, whose sequence is listed in Table 10. *TBP* was used as the reference gene to calculate fold change in the expression of MCTs. ΔCt values were first obtained: ΔCt= Threshold cycle (Ct) of *HPRT* - Ct of the gene. ΔΔCt values were then obtained: ΔΔCt=ΔCt of treated groups–ΔCt of untreated control groups. Fold change was calculated as 2-ΔΔCt, with control groups as 1- fold.

**Table 8. Volumes of RT-qPCR mixture used per each sample in evaluating MCTs expression.**

| | |
|---|---|
| **SYBR™ Green Master Mix** | 5µl |
| **Forward Primer** | 0.1µl |
| **Reverse Primer** | 0.1µl |
| **cDNA** | 1µl |
| **RNase-free water** | 3.8µl |
| **Total Volume** | **10µl** |

**Table 9. RT-qPCR amplification program using CFX96 Touch Real-Time PCR Detection System (Bio-Rad).**

| Step | Temperature (°C) | Duration | Cycles |
|---|---|---|---|
| **DNA Denaturation and Enzyme Activation** | 95 | 2min | 1 |
| **Denaturation** | 95 | 15s | 40 |
| **Annealing/Extension** | *MCT1* - 58<br>*MCT2* - 63<br>*MCT4* - 64<br>*TBP* - 60 | 1min | |
| **Melting Curve** | (a) | | |

(a) The determination of the thermal profile of the melting curve was achieved by monitoring changes in fluorescence intensity starting at 65°C during 5s and then, with a gradual increase in temperature until 95°C (0.5°C/s).

**Table 10. Sequence of the primers used in the RT-qPCR experiments.**

| Gene | Primer Sequence |
|---|---|
| ***MCT1*** | **Forward:** 5'-TTCCTCAGCCCTCTTTCAGA-3'<br>**Reverse:** 5'-GGTTACAGCGGACACTGGAT-3' |
| ***MCT2*** | **Forward:** 5'-AAGGCAAGAGCAAACTGCAT-3'<br>**Reverse:** 5'-AGTTCACGGTGCCTGGATAC-3' |
| ***MCT4*** | **Forward:** 5'-GCCACCTCAACGCCTGCTA-3<br>**Reverse:** 5'-TGTCGGGTACACCCATATCCTTA-3' |
| ***TBP*** | **Forward:** 5'-GGGAGAATCATGGACCAGAA-3'<br>**Reverse:** 5'-TTGCTGCTGCTGTCTTTGTT-3' |

## 3.13 ELISA

Enzyme-linked immunosorbent assay (ELISA) assay was used to assess the levels of the cytokines IL-10 and IL-1β on the supernatant of the co-culture experiments, using ELISA MAX™ Deluxe Set Mouse IL-10 (BioLegend®, #431414) and ELISA MAX™ Deluxe Set Mouse IL-1β (BioLegend®, #432604), according to manufacturer's instructions. In brief, one day before the ELISA assay was performed, 96-

well plates were coated with Capture antibody and allowed to rest overnight at 4°C. The following day, the wells were blocked by adding Assay Diluent and incubating during 1 hour at room temperature on a plate shaker. Plates were washed and then 100µl of the sample or diluted standards were added to the appropriate wells and incubated for 2 hours at room temperature with shaking. After that, detection antibody was added to each well and incubated for 1 hour at room temperature with shaking. Moreover, avidin-HRP was added to each well and incubated for 30 minutes at room temperature. A substrate solution was added to each well and incubated in the dark for 15 minutes. To conclude the assay, a stop solution was added to each well and the signal produced by the enzyme-substrate reaction was measured by the Thermo Scientific Varioskan® Flash readout at 570nm within 15 minutes after adding stop solution.

## 3.14 Small interfering RNA (siRNA) transfection

Small interfering RNA (siRNA) transfection was used to knockdown the expression of MCT2 on BMDM. Transfection experiments were performed using 45nM of MCT2 siRNA (Ambion®, #AM16704), as well as nontargeting scramble control (Ambion®, #AM4611), 3.5µl/ml of Lipofectamine RNAiMAX (Invitrogen, #13778075) and 150µl/ml of Opti-MEM. In brief, siRNA or scramble control, lipofectamine and Opti-MEM are added to one eppendorf tube, mixed and allowed to incubate for 5 minutes at room temperature. Approximately $2x10^6$ BMDM are seeded in 6-well plates and the content of the eppendorf tube is added to the appropriate wells. Knockdown efficiency was confirmed by Western Blot and total knockdown was only observed after 72 hours.

## 3.15 Statistical analysis

Statistical analysis was performed using Graph Pad Prism version 7. For statistical analysis of total cell biomass and quantification of glucose consumption and extracellular lactate, an unpaired two-tailed t-test was performed in order to compare the treated groups with the respective controls. All the data is reported as mean ± standard deviation and statistically significant differences were considered when p-value was lower than 0.05.

# CHAPTER 4 | RESULTS

## 4.1 Tumor-associated macrophages co-localized with MCT2

To evaluate the expression of MCTs on TAMs and adjacent cancer cells, we performed immunohistochemistry and immunofluorescence on paraffin-embedded tissue sections from Lewis lung carcinoma (LLC1) subcutaneous tumors in C57BL/6 mice. By immunohistochemistry we analyzed the expression of CD68, a glycoprotein highly expressed in macrophages. Expression of CD68 indicates the presence of macrophages within the tumor microenvironment (Figure 13A). Furthermore, by immunofluorescence we analyzed the expression of CD68 along with MCT1, MCT2 and MCT4 (Figure 13B-D). The results showed co-localization of macrophages (CD68+ cells) and MCT2 (Figure 13C), while MCT1 and MCT4 expression was found in cancer cells (CD68- cells). Since MCT1 and MCT4 isoforms are strongly associated with the export of lactate by highly glycolytic cancer cells[118], while MCT2 is responsible for the uptake of lactate[111], these results suggest the presence of a possible lactate shuttle between TAMs and cancer cells.

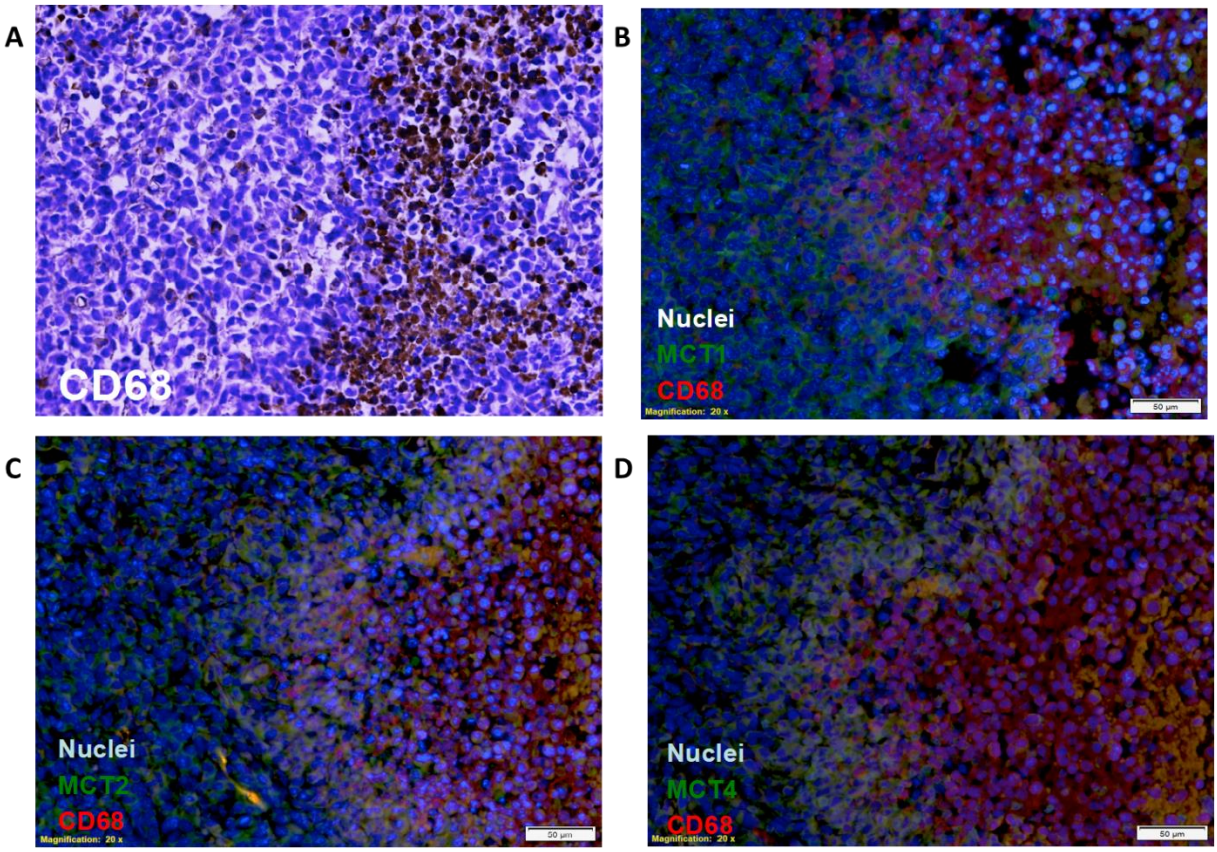


**Figure 13. Tumor-associated macrophages co-localized with MCT2. (A)** Immunohistochemistry staining for CD68 (in brown CD68 positive cells), a macrophage marker. **(B)** Immunofluorescence staining for MCT1 (green) and CD68 (red), **(C)** MCT2 (green) and CD68 (red), **(D)** MCT4 (green) and CD68 (red). The cell nucleus is counterstained with DAPI (blue). Immunofluorescence images were taken at 200x magnification.

## 4.2 Generation and characterization of MCT1 KO breast cancer cells

Since our aim was to disrupt lactate release from cancer cells, we first attempted to knockout MCT1 in the breast cancer cell line E0771 and in the lung cancer cell line LLC1 by using the CRISPR/Cas9 technology. After transfection, cells were treated with puromycin to enrich the pool of successfully transfected cells and sorted for the double expression of RFP/GFP by FACS. For the E0771 cells, RFP/GFP positive cells were single clone selected and seeded into a 96-well plate. Since LLC1 cells do not grow as single cells, 100 cells were selected and sorted into a 96-well plate. Different clones were collected and expanded for further characterization by Western blot. Although total MCT1 knockout was not achieved, it was possible to observe a decrease in MCT1 protein levels on the E0771 clone C1.51, when compared to the parental cell line E0771 wildtype (WT) (Figure 14A). To study the effect of MCT1 disruption on cell viability, we performed a Sulforhodamine B (SRB) assay. E0771 C1.51 cells, in standard DMEM medium (high glucose), displayed a significantly slower growth rate until 48 hours, when compared to E0771 parent cells, with a decrease in total cell biomass. However, between 48 and 72 hours E0771 C1.51 cells increased their growth rate and after 72 hours presented a significantly higher total cell biomass than the parental cells (Figure 14B). Since cancer cells possess the ability to switch their own metabolism, we further investigated if MCT1 disruption would make cells more sensitive to phenformin, a drug that inhibits the complex I of the respiratory chain in the mitochondria. Phenformin treatment had no effect on the growth rate of both E0771 C1.51 and parental cells (Figure 14B). Since glucose levels in solid tumors are known to be low and for further characterization, we incubated E0771 C1.51 and parental cells in DMEM low glucose (5mM), in an effort to resemble *in vivo* conditions. E0771 C1.51 cells displayed the same growth rate as parental cells, as cell viability increased until 48 hours but then the total cell biomass numbers decreased even below those observed at the beginning of the assay, suggesting cell death (Figure 14C). Once again, phenformin treatment had no effect on the growth rate of both cell lines (Figure 14C).

Regarding metabolism, E0771 C.1.51 cells only displayed a significant increase in glucose consumption when incubated in DMEM low glucose and DMEM low glucose with phenformin, compared to parental cells (Figure 14D). Phenformin treatment resulted in a significant increase of glucose consumption of both cell lines across the different conditions (Figure 14D). E0771 C1.51 cells not only increased lactate production when incubated in DMEM low glucose and DMEM low glucose with phenformin, but also upon phenformin treatment in standard DMEM medium (Figure 14E). In accordance to what we observed in Figure 14D, phenformin also increased the lactate production of both cell lines (Figure 14E). This can be explained due to the inhibition of the respiratory chain by phenformin, which

leads to a compensatory acceleration of glycolysis[165]. Unfortunately, for LLC1 cells, we were not able to obtain a negative population for MCT1. Thus, further experiments are necessary to maximize transfection efficiency. Overall, these results show that MCT1 disruption alters cell growth rate and increases glycolytic activity on low glucose conditions in E0771 cells.

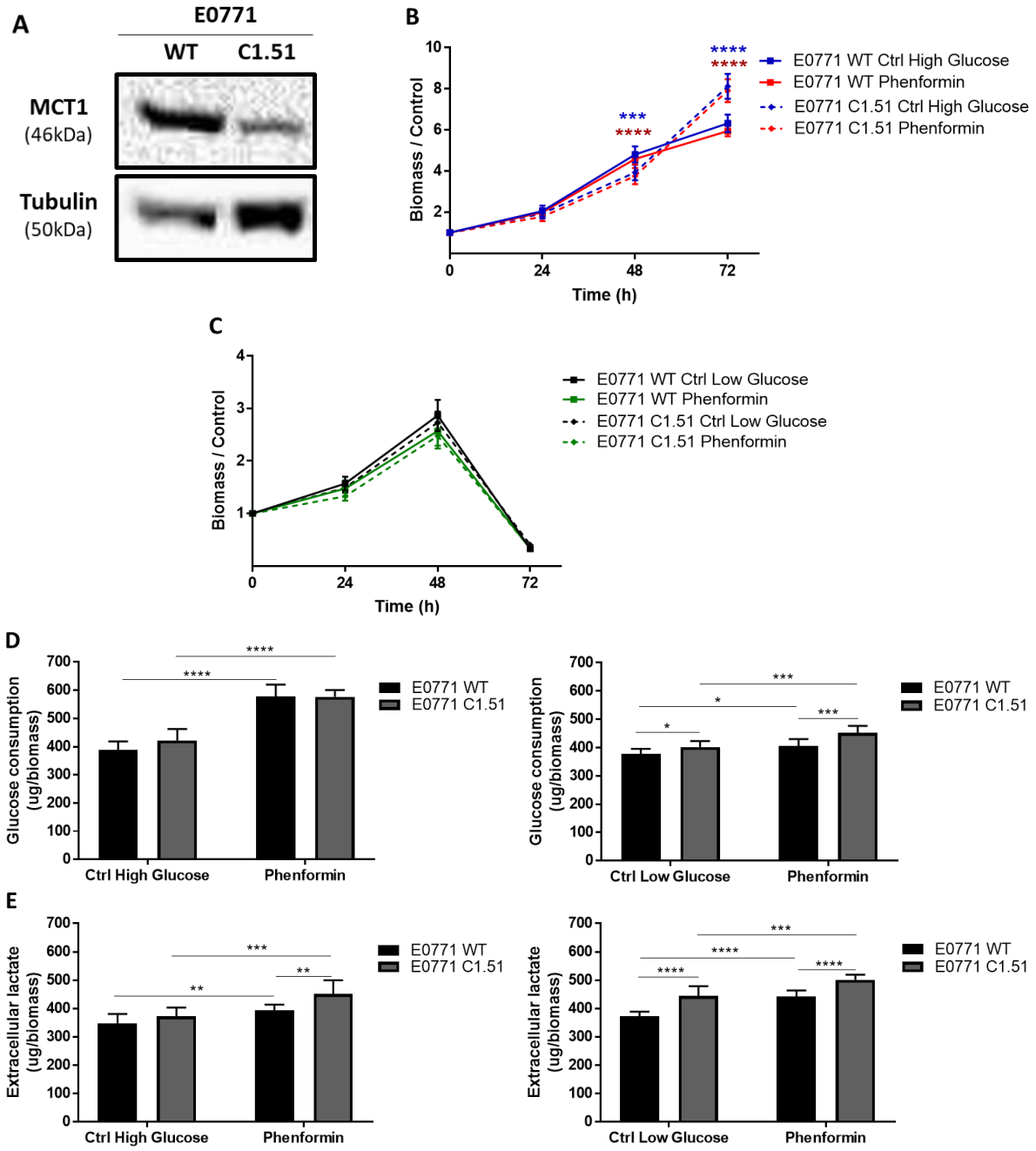


**Figure 14. Effect of MCT1 disruption in breast adenocarcinoma cell line E0771. (A)** Western blot analysis of MCT1 in E0771 WT and E0771 clone C1.51 cell lines. Tubulin was used as a loading control. **(B)** E0771 WT and E0771 C1.51 total cell biomass was assessed by Sulforhodamine B (SRB) assay after 24, 48 and 72 hours of incubation with 50μM of phenformin in DMEM high glucose (25mM) and in **(C)** DMEM low glucose (5mM). **(D)** Glucose consumption and **(E)** extracellular lactate quantification of E0771 WT and E0771 C1.51 cells after 24 hours of incubation with 50μM of phenformin in DMEM high and low glucose, using a commercial enzymatic kit. Results are displayed as mean ± standard deviation of three independent experiments with triplicates (* $p<0.05$; ** $p<0.01$; *** $p<0.001$; **** $p<0.0001$. Student's t-test was applied in the SRB assay and the glucose consumption and extracellular lactate quantification assay).

## 4.3 Generation and characterization of MCT4 KO breast cancer cells

Export of lactate can also be mediated by MCT4[111], therefore, we performed the knockout of MCT4 in the breast cancer cell line E0771 and in the lung cancer cell line LLC1 by using the CRISPR/Cas9 technology. The selection/sorter approaches were the same as mentioned for MCT1 KO and once again, we only succeeded to obtain E0771 KO cells. Full MCT4 knockout was achieved on the E0771 clone C4.14 cells, as no protein levels were detected by Western blot (Figure 15A). To investigate the effect of MCT4 knockout on cell viability, we performed the SRB assay. E0771 C4.14 cells, similar to what happened with E0771 C1.51 cells, displayed a slower growth rate when compared to E0771 parent cells, with a decrease in total cell biomass until 48 hours. However, between 48 and 72 hours E0771 C4.14 cells increase their growth rate and after 72 hours present a significantly higher total cell biomass than the parental cells (Figure 15B). Treatment with phenformin had no effect on the proliferation of both cell lines. Since it has already been described that MCT4 knockdown sensitizes cells to MCT1 inhibition[148], we further questioned if concomitant inhibition of MCT1 and MCT4 would increase cells sensitivity towards phenformin. For that purpose, we treated both cell lines with the combination of the MCT1 inhibitor AZD3965 and phenformin (Figure 15C). Treatment with AZD3965 and its combination with phenformin had no effect on E0771 WT cells, however, it hindered the growth of E0771 C4.14 cells (Figure 15C). The significant decrease on cell biomass of E0771 C4.14 cells upon combination of AZD3965 with phenformin was mainly caused by inhibition of both MCT1 and MCT4, since no differences were observed on cell biomass between AZD3965 and its combination with phenformin (Figure 15C). These interesting results assert that MCT4 function is compromised in E0771 C4.14 cells and blocking both MCT1 and MCT4 is sufficient to inhibit cells growth.

Treatment with phenformin, AZD3965, or their combination had no significant effect on glucose consumption of both cell lines (Figure 15D). However, E0771 C4.14 cells treated with AZD3965 and combination of AZD3965 with phenformin displayed a significant decrease in lactate production, when compared to E0771 WT and E0771 C4.14 control cells, demonstrating the importance of MCT1 and MCT4 for lactate export (Figure 15E).

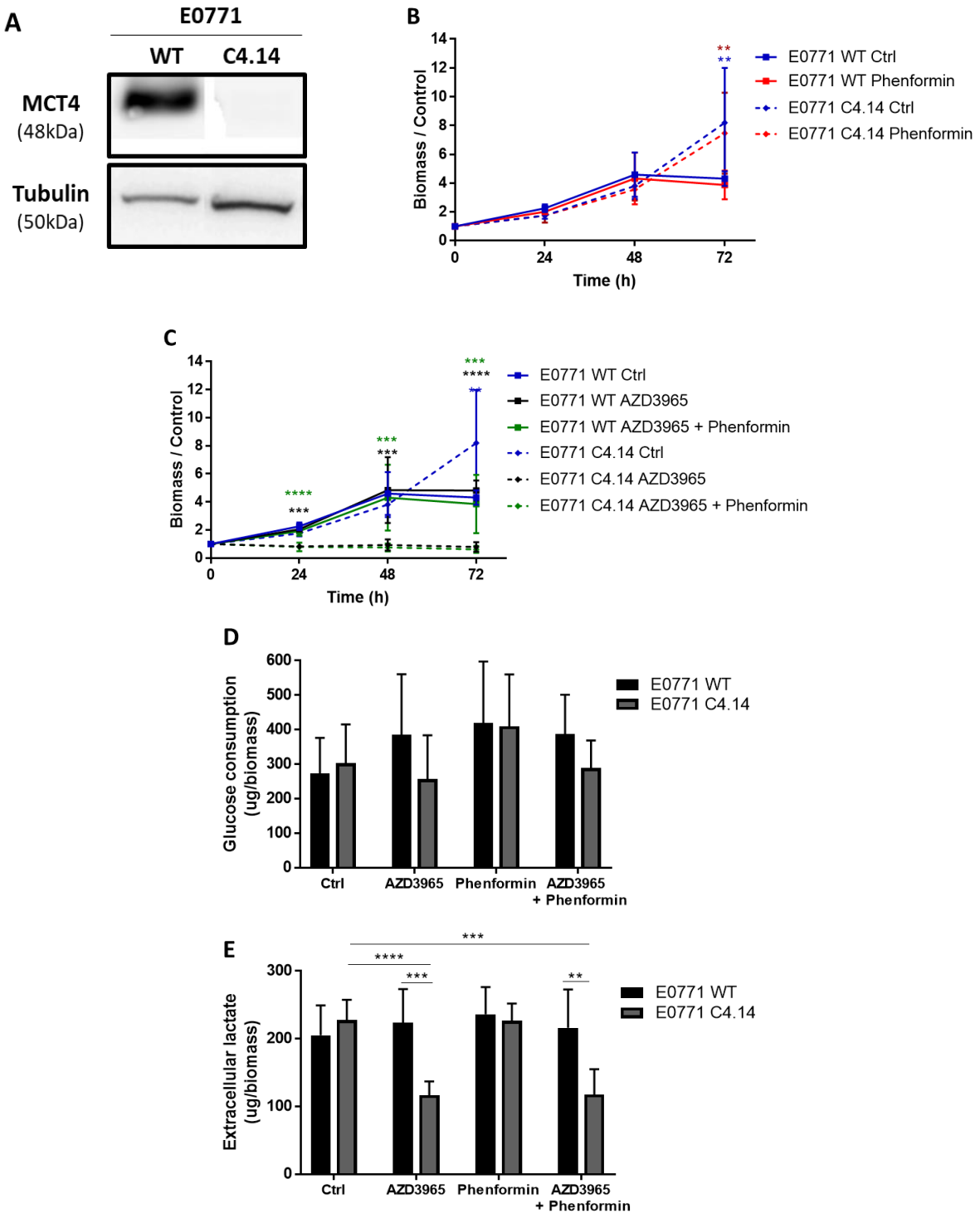


**Figure 15. Effect of MCT4 disruption in breast adenocarcinoma cell line E0771. (A)** Western blot analysis of MCT4 in E0771 WT and E0771 clone C4.14 cell lines. Tubulin was used as a loading control. **(B)** E0771 WT and E0771 C4.14 cell viability was assessed by Sulforhodamine B (SRB) assay after 24, 48 and 72 hours of incubation with 50µM of phenformin and **(C)** with 300nM of MCT1/2 inhibitor AZD3965 alone or in combination with 50µM of phenformin. **(D)** Glucose consumption and **(E)** extracellular lactate quantification of E0771 WT and E0771 C4.14 cells after 24 hours of incubation with 50µM of phenformin, 300nM of AZD3965 or a combination of both, using a commercial enzymatic kit. Results are displayed as mean ± standard deviation of three independent experiments with triplicates (* $p<0.05$; ** $p<0.01$; *** $p<0.001$; **** $p<0.0001$. Student's t-test was applied in the SRB assay and the glucose consumption and extracellular lactate quantification assay).

## 4.4 Single targeting MCT1/4 was not able to polarize macrophages towards a pro-inflammatory phenotype

Evidence indicates that tumor-derived lactate modulates immune cell function and cytokine production, serving as a negative feedback signal to create an immunosuppressive TME. To evaluate the effect of disrupting lactate release from tumor cells on TAMs polarization, we performed co-culture experiments where we used bone marrow-derived macrophages and the E0771 C1.51 and E0771 C4.14 cells, from now referred as MCT1 KO cells and MCT4 KO cells, respectively, for a better understanding. We evaluated the expression of M1-like and M2-like macrophage phenotype associated genes, namely *Nos2* and *Ccl2* (M1-like phenotype) and *Arg1* and *Chi3l3* (M2-like phenotype). We observed that MCT1 KO cells (Figure 16A) and MCT4 KO cells (Figure 16B) display a tendency to induce the expression of both M1-like and M2-like associated genes in macrophages, when compared to E0771 WT cells. We further evaluated the production of the anti-inflammatory cytokine IL-10 and the pro-inflammatory cytokine IL-1β by an ELISA assay in order to understand if disruption of lactate export could alter cytokine production by macrophages. The results suggest that macrophages, upon co-culture with MCT1 KO cells, increase the production of IL-10 but no effect was observed in IL-1β (Figure 16C), whereas no effects were found for IL-10 and IL-1β production on the co-culture of macrophages with MCT4 KO cells (Figure 16D). The data suggests that disrupting lactate release from cancer cells by single target of MCT1 or MCT4 was not able to polarize macrophages towards a pro-inflammatory phenotype.

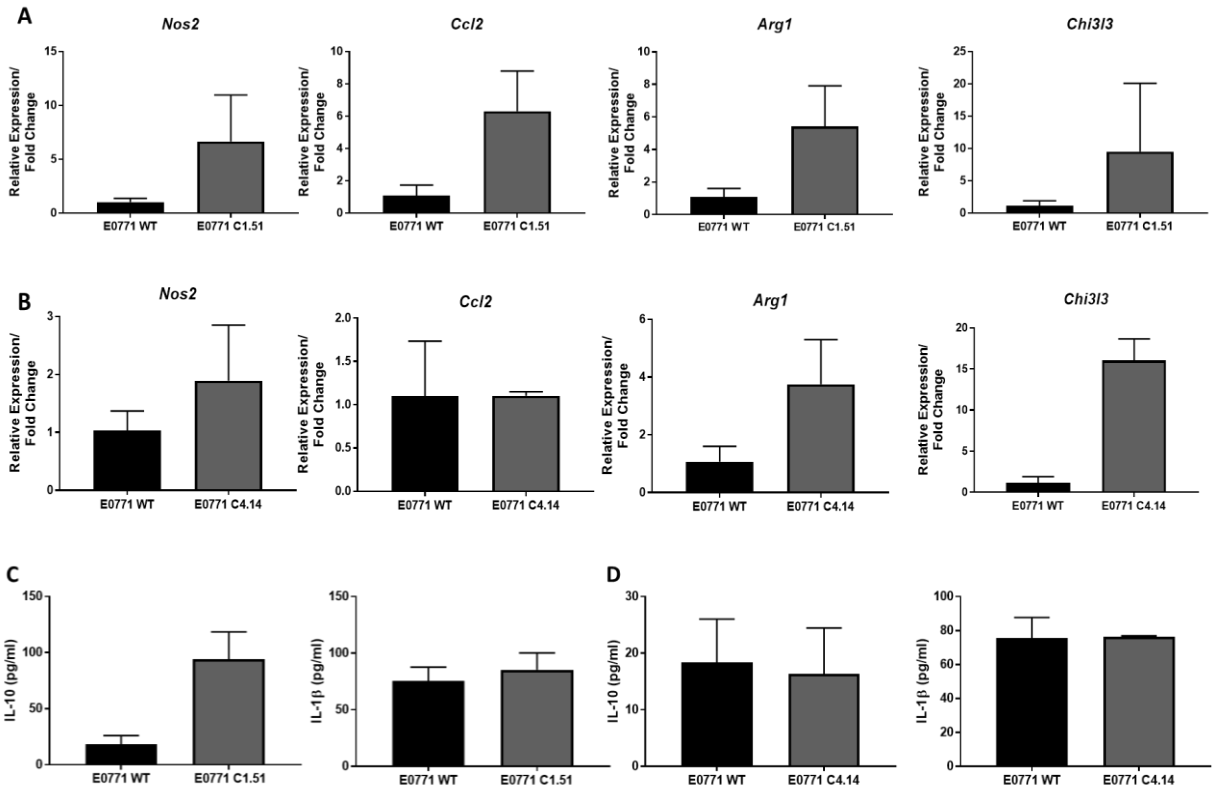


**Figure 16. Single targeting of MCT1/4 was not able to polarize macrophages towards a pro-inflammatory phenotype.** Expression levels of *Nos2*, *Ccl2*, *Arg1* and *Chi3l3* genes in **(A)** macrophages co-cultured with E0771 WT and E0771 C1.51 cells for 24 hours and **(B)** macrophages co-cultured with E0771 WT and E0771 C4.14 cells for 24 hours were determined by RT-qPCR and normalized to the expression of *Hprt*. IL-10 and IL-1β cytokine levels in **(C)** macrophages co-cultured with E0771 WT and E0771 C1.51 cells for 24 hours and **(D)** macrophages co-cultured with E0771 WT and E0771 C4.14 cells for 24 hours were determined by ELISA assay. Results are displayed as mean ± standard deviation of one independent experiment with duplicates.

## 4.5 Targeting MCT2 inhibited the M2-like phenotype of macrophages

We have previously observed that disrupting lactate release from cancer cells by single targeting MCT1 or MCT4 did not polarize macrophages towards an anti-tumoral phenotype. Considering the lactate shuttle hypothesis, lactate released to the extracellular medium is imported by TAMs and induces polarization of TAMs into a M2-like phenotype[108,109]. Thus, we hypothesized if inhibiting the uptake of lactate by macrophages, it would revert the pro-tumoral phenotype displayed. To do so, we first started by performing a co-culture of macrophages with LLC1 cells to evaluate the role of tumor cells on macrophages polarization and expression of MCTs. We evaluated the expression of M1-like and M2-like macrophage phenotype associated genes, namely *Nos2*, *Ccl2* and *Tnf* (M1-like phenotype) and *Arg1*, *Chi3l3* and *CD163* (M2-like phenotype). Macrophages co-cultured with LLC1 display a tendency to increase the expression of the M2-like genes *Arg1* and *CD163* and the expression of the M1-like gene *Nos2* (Figure 17A). Furthermore, exposure to LLC1 cells increased the expression of MCT2 in macrophages (Figure 17B). Since MCT2 is responsible for the uptake of lactate[111], this could indicate a possible metabolic symbiosis between cancer cells and macrophages through lactate shuttle, where lactate is released by LLC1 cells and consumed by macrophages via MCT2. Therefore, to understand the role of MCT2 on this metabolic symbiosis, we performed a knockdown for MCT2 in macrophages using a small interfering RNA (siRNA) (Figure 17C). Knockdown of MCT2 suggests an inhibition of the M2-like phenotype of macrophages in co-culture with LLC1 cells, compared to scramble control, with a tendency to decrease the expression of the *Chi3l3* and *CD163 genes* (Figure 17D). These results suggest that MCT2 plays a crucial role in the lactate shuttling between cancer cells and macrophages and targeting MCT2 possibly inhibits the pro-tumoral phenotype of macrophages.

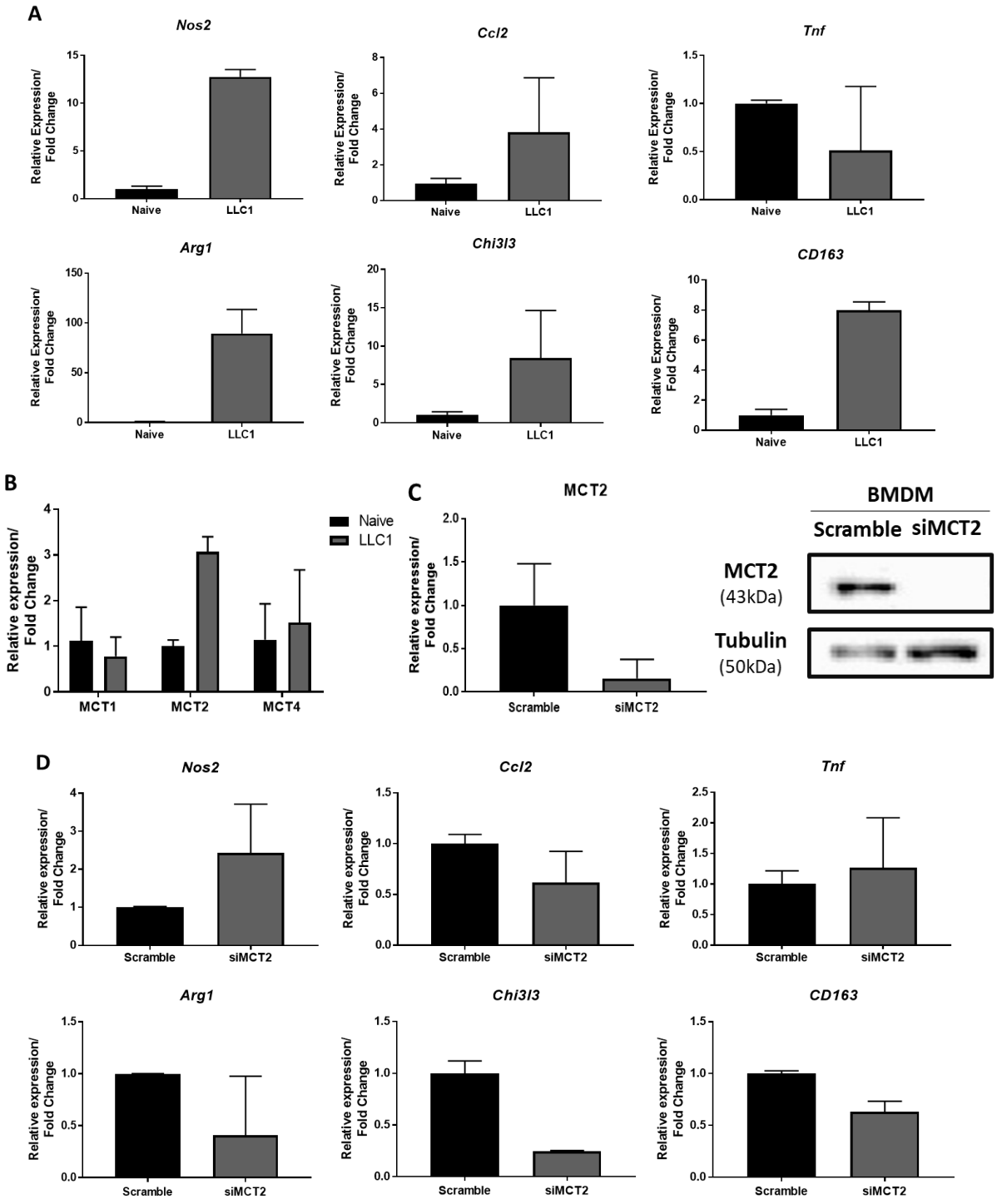


**Figure 17. Targeting MCT2 inhibits the M2-like phenotype of macrophages. (A)** Expression levels of *Nos2*, *Ccl2*, *TNF*, *Arg1*, *Chi3l3* and *CD163* genes in naive macrophages and macrophages co-cultured with LLC1 cells for 24 hours were evaluated by RT-qPCR and normalized to the expression of *Hprt*. **(B)** Expression levels of *MCT1*, *MCT2* and *MCT4* in naive macrophages and macrophages co-cultured with LLC1 cells for 24 hours were evaluated by RT-qPCR and normalized to the expression of *Tbp*. **(C)** Expression levels of *MCT2* in macrophages transfected with siRNA targeting MCT2. Expression levels of *MCT2* were normalized to the expression of *Tbp* and Tubulin was used as loading control in the Western Blot. **(D)** Expression levels of *Nos2*, *Ccl2*, *TNF*, *Arg1*, *Chi3l3* and *CD163* genes in macrophages transfected with siMCT2 and scramble control co-cultured with LLC1 cells for 24 hours were evaluated by RT-qPCR and normalized to the expression of *Hprt*. Results are displayed as mean ± standard deviation of two independent experiments.

# CHAPTER 5 | DISCUSSION

The discovery of oncogenes, tumor suppressor genes and the study of the mechanisms involved in genomic alterations implicated in cancer, dominated the focus of cancer research for many decades[166]. As the understanding of malignant transformation grew, it became evident that solely alterations to the genome were not sufficient to explain tumor growth and metastasis. This realization increased the interest in understanding cancer cell metabolism, first described by Otto Warburg in the 1920s[5]. Over the last decades, several studies report the link between metabolic remodeling and tumor growth and in 2011, the reprogramming of cellular energy metabolism was recognized as a hallmark of cancer cells[8] . The altered metabolism of cancer cells confers a selective advantage over normal cells, promoting their survival and proliferation[9].

Lactate, the end product of glycolysis, is produced in large excess by cancer cells and is drawing increased attention of the cancer research community, due to its role as a metabolic modulator of different cancer features including cell migration and invasion, sustained angiogenesis, reprogramming of energy metabolism and evasion of immune surveillance[44–47]. The discovery of lactate shuttles between cancer cells and non-malignant cells from the TME hypothesized that lactate exported by cancer cells is imported and re-used by immune cells. Evidence indicates that high levels of extracellular lactate influence immune cell metabolism and cytokine production and may serve as a negative feedback signal, limiting inflammation[51–55]. Indeed, lactate has been reported to induce M2-like polarization of TAMs, who contribute to tumor progression by promoting angiogenesis, metastasis and immunosuppression[93,105]. Taking into consideration MCT1 and MCT4 overexpression in cancer cells and its crucial role in the maintenance of their glycolytic metabolism[118], we envisioned that disrupting the lactate release from cancer cells could be a promising approach to revert the pro-tumoral phenotype of TAMs.

For that purpose, we first attempted to understand the expression pattern of MCTs on TAMs and cancer cells in a subcutaneous murine Lewis lung carcinoma (LLC1) model. By immunohistochemistry analysis we confirmed the expression of CD68, a glycoprotein highly expressed in macrophages[167], indicating the presence of TAMs on the tumor microenvironment, in agreement to what is described in the literature[168] (Figure 13A). Furthermore, by immunofluorescence, we observed a co-localization of CD68 with the MCT2 isoform, while MCT1 and MCT4 are mainly expressed in CD68- cells (Figure 13B-D). Since MCT1 and MCT4 are reported to be able to export lactate and MCT2 is responsible for the uptake of lactate[111], these results are in accordance with the lactate shuttle hypothesis, in which cancer cells export

lactate via MCT1 or MCT4 and TAMs can import lactate via MCT2. In order to support this hypothesis, these experiments should be extended to other cancer models.

Bearing the previous results in mind, we tried to disrupt lactate release from cancer cells, by knocking out MCTs, using the CRISPR/Cas9 technology. The tumor-supporting function of TAMs have been reported in several types of cancer, such as lung and breast cancer [169,170]. Besides LLC1 cells, we also used the breast adenocarcinoma E0771 cell line, which originates highly aggressive tumors with reports of an immunosuppressive microenvironment[171]. Both cell lines were used during this work, but unfortunately, a successful transfection using CRISPR/Cas9 was only achieved with the E0771 cell line, as LLC1 cells were very hard to transfect, hence the reason why we display results with two different cell lines. In the future, we intend to perform these experiments with both cell lines, and for that reason, further optimization of the protocols is needed.

We first started by knocking out MCT1 on cancer cells, and although total knockout of MCT1 was not achieved, we were able to observe a decrease in the protein levels of MCT1 on E0771 clone C1.51 cells (Figure 14A). A possible explanation for this result is a lack of efficiency of the CRISPR machinery or the delivery method used to transfect these cells, as CRISPR efficiency will vary based on the method of delivery and cell type[154]. Moreover, cells were sorted by the expression of fluorescent tagged proteins RFP and GFP. The use of a specific antibody for MCT1 and MCT4 to select negative cells could be a better approach. However, the commercially available antibodies for MCT1 and MCT4 correspond to epitopes within the C-terminal cytoplasmic domain of these transporters. Based on this, for live sorting of MCT1 and MCT4-null cells using antibodies, a permeabilization step would be required and this leads to cell death, making this process unviable. In the future, it will be important a further optimization of the protocol or the use of another CRISPR/Cas9 KO Plasmids. We next characterized the effect of MCT1 disruption in cell viability and the glucose metabolism of these cells. MCT1 disruption altered the cell growth rate of E0771 cells (Figure 14B). In low glucose conditions, MCT1 KO cells displayed the same cell growth rate as parental cells, with cell death after 48 hours, possibly due to the low glucose availability in the medium. Blockage of MCTs has been reported to cause a shift in cancer metabolism from glycolysis to OXPHOS, sensitizing them to phenformin[172,173], a biguanide drug that inhibits the complex I of the respiratory chain in the mitochondria. Thus, we further investigated if MCT1 disruption would sensitize cells to phenformin. Treatment with phenformin had no effect on cell viability (Figure 14B and C), suggesting that cells still rely on the glycolytic pathway for proliferation. In contrast with our results, a study from Hong, et al., demonstrated that MCT1 knockdown by short hairpin RNA (shRNA) or MCT1 inhibition by AZD3965 in

the glycolytic breast cancer cell lines HS578T, SUM149PT and SUM159PT, with dual MCT1/MCT4 expression, decreased cell proliferation during a 5-day period. The decrease in cell proliferation was rescued by the expression of shRNA-resistant MCT1 cDNA, showing that MCT1 is crucial for the proliferation of glycolytic breast cancer cells[174]. Our results can be explained by the incomplete knockout of MCT1 (Figure 14A) and the functional redundancy between MCT1 and MCT4 allows MCT4 compensation when MCT1 is disturbed[145], therefore further analysis of MCT4 expression is needed to clarify these results. Regarding the metabolic profile, the same authors showed that MCT1 knockdown or inhibition enhanced an oxidative metabolism and reduced pyruvate but not lactate export, with no alterations of MCT4 protein levels, suggesting that MCT1 could possibly mediate pyruvate export[174]. E0771 WT cells, upon phenformin treatment, increased their glucose consumption and lactate production in standard DMEM medium and low glucose DMEM, suggesting that although it has no effect on cell proliferation, inhibition of the respiratory chain increases the glycolytic flux of these cells (Figure 14D and E). The disruption of MCT1, in accordance to Hong et al.[174], was not able to decrease the export of lactate or even the consumption of glucose by E0771 cells, in both standard DMEM medium and low glucose DMEM. Furthermore, MCT1 KO cells treatment with phenformin also increased their glycolytic flux (Figure 14D and E). This inability to decrease the export of lactate might be due to an overcompensation of the expression of MCT4, as it has already been described[145], but once again, further analysis of MCT4 expression is needed to justify these results. It would also be interesting to evaluate the pyruvate export rate, since MCT1 is important to ensure a NADH/NAD+ redox state equilibrium between cells due to its ability to transport pyruvate and lactate[111]. The fact that MCT1 knockout was not fully achieved can have an impact on these results, and therefore, these characterization experiments need to be redone once the full knockout of MCT1 is successfully achieved.

Besides MCT1, MCT4 is also able to export lactate into the extracellular milieu[111], therefore, the next step was to try to knockout MCT4 on cancer cells using the CRISPR/Cas9 technology. Unlike MCT1, no MCT4 protein levels were detected on E0771 clone C4.14 cells, indicating a full MCT4 knockout (Figure 15A). MCT4 knockout also altered cell growth rate of E0771 cells and phenformin had no effect on cell viability (Figure 15B). Despite the growth behavior displayed by E0771 WT cells in control conditions in Figure 15B and 14B is different, the fact that phenformin had no effect on cell growth rate on both occasions suggests that E0771 cells rely on the glycolytic pathway for their proliferation and the altered cell growth rate is possibly due to the increasing number of passages. It is known that MCT4 knockdown sensitizes cells to MCT1 pharmacological inhibition[148], therefore we treated E0771 WT and E0771 C4.14 cells with the specific MCT1 inhibitor AZD3965. As stated before, in the study presented

by Hong et al., MCT1 inhibition induced an oxidative metabolism and reduced proliferation. Besides that, dual treatment of AZD3965 with phenformin further reduced proliferation rates by blocking the switch to oxidative metabolism[174]. Treatment of E0771 WT cells with MCT1 inhibitor plus the combination with phenformin had no effect on the cell growth rate, suggesting that the glycolytic pathway, presumably maintained by MCT4 lactate exportation, allows cancer cell proliferation. Consistent with this notion, treatment of MCT4 KO cells with MCT1 inhibitor hindered their cell growth (Figure 15C). Based on these results, it seems E0771 cells are not able to change their metabolic profile towards OXPHOS to support proliferation, as concomitant inhibition of MCT1 and MCT4, impairing the lactate export, was sufficient to reduce cell viability, supporting the evidence that blockade of lactate export inhibits cancer cell proliferation[134,175]. Similar to what we observed MCT1 KO cells, pharmacological inhibition of MCT1 was not able to reduce the glycolytic flux, as treatment of E0771 WT cells with AZD3965 resulted in no significant differences on glucose consumption and lactate production (Figure 15D and E), indicating that single target of MCT1 is not sufficient to block the export of lactate by E0771 cells. Metabolic analysis of MCT4 KO cells also revealed that single target of MCT4 was not able to decrease the export of lactate and the consumption of glucose, when compared with E0771 WT cells (Figure 15D and E). However, in MCT4 KO cells, upon treatment with MCT1 inhibitor, was possible to observe a tendency for the decrease of glucose consumption and the production of lactate was significantly impaired (Figure 15D and E), supporting the evidence that blockade of lactate export leads to an inhibition of the glycolytic pathway[173] and E0771 cells rely on the glycolytic pathway for their proliferation. These results indicate a functional redundancy between MCT1 and MCT4 in E0771 cells, as only the dual target of these transporters is capable of blocking the export of lactate and consequently impair cell growth.

Tumor-derived lactate has been reported to induce a M2-like polarization in TAMs[104,105,109], so the next question addressed was whether the disruption of lactate release from cancer cells could revert the pro-tumoral phenotype displayed by TAMs. By co-culture of macrophages with MCT1 KO and MCT4 KO cells, we observed that both cell lines display a tendency to increase the expression of both M1-like and M2-like gene markers, when compared to WT cells (Figure 16A and B). These results can be explained by the fact that MCT1 and MCT4 KO cells are still able to produce lactate (Figure 14E and 15E), and preliminary non-published results from our team demonstrate that lactate is able to induce the expression of both M1-like and M2-like gene markers, although some studies have reported that lactate only increases the expression of M2-like gene markers[104,105]. Furthermore, analysis of the production of cytokines IL-10 and IL-1β showed that MCT4 disruption had no effect on cytokine production, while co-culture of macrophages with MCT1 KO cells suggest that macrophages increase the production of IL-10

(Figure 16C). Once again, a possible explanation for these results is the fact that MCT1 KO cells still export lactate and macrophages stimulated with lactate or in co-culture with cancer cells have been shown to increase the production of IL-10[176,177]. These results suggest that blocking lactate export in cancer cells by single targeting MCT1 or MCT4 was not able to polarize macrophages towards an anti-tumoral phenotype. Since a reduction in the export of lactate was only observed in MCT4 KO cells treated with MCT1 inhibitor, it would be of interest to perform a co-culture of macrophages with MCT4 KO cells pre-treated with AZD3965 and evaluate if the reduction of lactate export could impact the polarization and cytokine production of macrophages.

The lactate shuttle hypothesis indicates that lactate exported by the cancer cells to the TME is imported by TAMs, which will promote TAMs polarization towards an M2-like phenotype and contribute to tumor progression. Since the previous results demonstrated that single target of MCT1 or MCT4 in cancer cells was not able to polarize macrophages towards a pro-inflammatory phenotype, we though that inhibition of the uptake of lactate by TAMs could revert the pro-tumoral phenotype displayed. Co-culture experiments showed that BMDM exposed to LLC1 cells display a tendency to increase the expression of *Arg1, CD163* and *Nos2* (Figure 17A). The increase in the expression of *Arg1* is consistent with a study from Colegio et al., in which TAMs from LLC1 tumors expressed high levels of *Arg1* and BMDM stimulated with LLC1-conditioned medium also increased the expression of *Arg1*[105]*.* Other studies reported that BMDM stimulated with LLC1-conditioned medium and direct co-culture of LLC1 cells with the macrophage cell line U937 increased the chemokine CCL2 production[178,179]. Yet, in our results, no statistical significances were detected in *Ccl2* mRNA levels. However, the increased expression of *Nos2* in our results is unexpected based on the fact that both *Nos2* and *Arg1* enzymes share the same substrate, arginine, and upregulation of *Arg1* is reported to prevent *Nos2* activity[180]. Still, this mixed M1/M2 phenotype displayed by macrophages has already been reported in colorectal cancer and pancreatic ductal adenocarcinoma. Stimulation of the monocytic cell line THP-1 with the colorectal cancer cell lines HCT116 or HT-29-conditioned medium resulted in an increase in the production of both pro-inflammatory cytokines IFN-γ, IL-1β and TNF-α, and anti-inflammatory cytokine IL-10, and increased the expression of the M2-like gene marker *CD163*[81]. Similarly, stimulation of peripheral blood monocytes with the pancreatic ductal adenocarcinoma cell lines Panc1 and MiaPaCa2-conditioned medium increased the expression of M1-like gene markers *IL-1β, IL-6* and *TNF-α,* and also the M2-like gene markers *Arg1* and *IL-10*[82]*.* Despite this mixed phenotype, in both studies macrophages promoted metastasis and EMT. In our results, co-culture of macrophages with LLC1 cells also showed a tendency to increase the expression of MCT2 in macrophages (Figure 17B). This increase in the expression of MCT2 in macrophages is in

accordance with what we observed in the immunofluorescence analysis of LLC1 tumors (Figure 13C). Bearing in mind that MCT2 is responsible for the uptake of lactate[111], these evidence indicates a possible metabolic symbiosis between LLC1 cells and macrophages through lactate shuttle, where lactate is released by LLC1 cells and consumed by macrophages via MCT2. In fact, a study in bladder cancer cells already demonstrated that blockage of MCTs, by using quercetin, was able to inhibit the M2-like phenotype of macrophages[109]. Therefore, we focused our attention on MCT2 and, in order to understand the role that MCT2 plays in this metabolic symbiosis, we performed an MCT2 knockdown in macrophages (Figure 17C). Interestingly, the knockdown of MCT2 resulted in a tendency to decrease the expression of the M2-like gene markers *CD163* and *Chi3l3,* upon co-culture with LLC1 cells (Figure 17D). Further experiments are needed in order to confirm these results. These promising results suggest that MCT2 is crucial to this metabolic interplay between cancer cells and macrophages and targeting MCT2 possibly inhibits the pro-tumoral phenotype of macrophages.

# CHAPTER 6 | CONCLUDING REMARKS AND FUTURE PERSPECTIVES

In this master thesis, we were able to identify a possible metabolic symbiosis between cancer cells and tumor associated macrophages in a murine lung cancer model. Combination of MCT4 knockout with pharmacological inhibition of MCT1 resulted in a decrease of lactate export and cell viability, indicating the importance of the glycolytic pathway to the survival of cancer cells. Furthermore, single targeting MCT1 and MCT4 was not able to disrupt the total lactate export by cancer cells and therefore, we could not reprogram macrophages towards an anti-tumoral phenotype. Interestingly, we highlighted the role of MCT2 in the lactate shuttling between cancer cells and macrophages, as co-culture with cancer cells increased the expression of MCT2 in macrophages and knockdown of MCT2 in macrophages inhibited its pro-tumoral phenotype. Although our goal of blocking lactate export by genetically knocking out MCTs was not achieved, our findings assert that a single MCT isoform knockout is not sufficient and therefore, in the future, a double knockout for MCT1/MCT4 on cancer cells should be performed, or knockout its ancillary protein CD147, as it has already been described by our team that disruption of CD147 decreased MCT1 and MCT4 expression and activity[172]. After the genetic modification desired is validated, metabolic characterization of these genetically engineered cells could be performed by using commercial enzymatic assays for glucose and lactate quantification. One limitation of the *in vitro* transwell co-culture system is that only investigates the effect of soluble secretions between two cell types. Therefore, due to complexity of the tumor microenvironment, it would be of interest to investigate the *in vivo* role of MCTs on cancer initiation and how disrupting lactate efflux to the TME influences innate and adaptive immune cells recruitment and function. To do so, C57BL/6 mice could be injected with genetically modified cancer cells and characterization of immune cells populations inside the TME performed by flow cytometry analysis. Moreover, growing evidence proposes that TAMs profile and function can be characterized by their metabolic phenotype, therefore it would be of interest to isolate TAMs from the tumor mass with the help of magnetic microbeads or FACS and further evaluate their metabolic phenotype.

This master thesis provided further insights into the mechanism of the lactate circuits in tumors, which are still poorly understood, due to the complexity of the tumor microenvironment and the interconnections between the cells involved.

## CHAPTER 7 | BIBLIOGRAPHY


1. Global Health Estimates 2016. Disease burden by Cause, Age, Sex, by Country and by Region, 2000-2016. *Geneva, World Health Organization* (2018).

2. Bray, F. *et al.* Global cancer statistics 2018: GLOBOCAN estimates of incidence and mortality worldwide for 36 cancers in 185 countries. *CA. Cancer J. Clin.* **68,** 394–424 (2018).

3. De Berardinis, R. J. & Chandel, N. S. Fundamentals of cancer metabolism. *Sci. Adv.* **2,** e1600200 (2016).

4. Akram, M. Mini-review on glycolysis and cancer. *J. Cancer Educ.* **28,** 454–457 (2013).

5. Warburg, O. The metabolism of carcinoma cells. *J. Cancer Res.* **9,** 148–163 (1925).

6. Kim, J. W. & Dang, C. V. Cancer's molecular sweet tooth and the warburg effect. *Cancer Res.* **66,** 8927–8930 (2006).

7. Vazquez, A., Liu, J., Zhou, Y. & Oltvai, Z. N. Catabolic efficiency of aerobic glycolysis: The Warburg effect revisited. *BMC Syst. Biol.* **4,** 58 (2010).

8. Hanahan, D. & Weinberg, R. A. Hallmarks of cancer: The next generation. *Cell* **144,** 646–674 (2011).

9. Boroughs, L. K. & Deberardinis, R. J. Metabolic pathways promoting cancer cell survival and growth. *Nat. Cell Biol.* **17,** 351–359 (2015).

10. Ahn, C. S. & Metallo, C. M. Mitochondria as biosynthetic factories for cancer proliferation. *Cancer Metab.* **3,** 1 (2015).

11. Ramakrishnan, N., Chen, R., McClain, D. E. & Bünger, R. Pyruvate prevents hydrogen peroxide-induced apoptosis. *Free Radic. Res.* **29,** 283–295 (1998).

12. Miwa, H., Fujii, J., Kanno, H., Taniguchi, N. & Aozasa, K. Pyruvate secreted by human lymphoid cell lines protects cells from hydrogen peroxide mediated cell death. *Free Radic. Res.* **33,** 45–56 (2000).

13. Kim, S. Y. Cancer energy metabolism: Shutting power off cancer factory. *Biomol. Ther.* **26,** 39–44 (2018).

14. Moreno-Sánchez, R., Rodríguez-Enríquez, S., Marín-Hernández, A. & Saavedra, E. Energy metabolism in tumor cells. *FEBS J.* **274,** 1393–1418 (2007).

15. Majmundar, A. J., Wong, W. J. & Simon, M. C. Hypoxia-Inducible Factors and the Response to Hypoxic Stress. *Mol. Cell* **40,** 294–309 (2010).

16. Porporato, P. E., Dhup, S., Dadhich, R. K., Copetti, T. & Sonveaux, P. Anticancer targets in the glycolytic metabolism of tumors: A comprehensive review. *Front. Pharmacol.* **2,** 49 (2011).

17. Hayashi, M. *et al.* Induction of glucose transporter 1 expression through hypoxia-inducible factor 1alpha under hypoxic conditions in trophoblast-derived cells. *J. Endocrinol.* **183,** 145–54 (2004).

18. Labak, C. M. *et al.* Glucose transport: Meeting the metabolic demands of cancer, and applications in glioblastoma treatment. *Am. J. Cancer Res.* **6,** 1599–1608 (2016).

19. Lu, H., Forbes, R. A. & Verma, A. Hypoxia-inducible factor 1 activation by aerobic glycolysis implicates the Warburg effect in carcinogenesis. *J. Biol. Chem.* **277,** 23111–23115 (2002).

20. Rawat, D. *et al.* Lactate as a signaling molecule: Journey from dead end product of glycolysis to tumor survival. *Front. Biosci. - Landmark* **24,** 366–381 (2019).

21. Thangaraju, M., Carswell, K. N., Prasad, P. D. & Ganapathy, V. Colon cancer cells maintain low levels of pyruvate to avoid cell death caused by inhibition of HDAC1/HDAC3. *Biochem. J.* **417,** 379–389 (2009).

22. Koukourakis, M. I., Giatromanolaki, A. & Sivridis, E. Lactate dehydrogenase isoenzymes 1 and 5: Differential expression by neoplastic and stromal cells in non-small cell lung cancer and other epithelial malignant tumors. *Tumor Biol.* **24,** 199–202 (2003).

23. Shim, H. *et al.* c-Myc transactivation of LDH-A: Implications for tumor metabolism and growth. *Proc. Natl. Acad. Sci. U. S. A.* **94,** 6658–6663 (1997).

24. Fantin, V. R., St-Pierre, J. & Leder, P. Attenuation of LDH-A expression uncovers a link between glycolysis, mitochondrial physiology, and tumor maintenance. *Cancer Cell* **9,** 425–434 (2006).

25. Fan, J. *et al.* Tyrosine Phosphorylation of Lactate Dehydrogenase A Is Important for NADH/NAD+ Redox Homeostasis in Cancer Cells. *Mol. Cell. Biol.* **31,** 4938–4950 (2011).

26. Granchi, C., Bertini, S., Macchia, M. & Minutolo, F. Inhibitors of Lactate Dehydrogenase Isoforms and their Therapeutic Potentials. *Curr. Med. Chem.* **17,** 672–697 (2010).

27. Giatromanolaki, A. *et al.* Lactate dehydrogenase 5 (LDH-5) expression in endometrial cancer relates to the activated VEGF/VEGFR2(KDR) pathway and prognosis. *Gynecol. Oncol.* **103,** 912–918 (2006).

28. Jiang, F., Ma, S., Xue, Y., Hou, J. & Zhang, Y. LDH-A promotes malignant progression via activation of epithelial-to-mesenchymal transition and conferring stemness in muscle-invasive bladder cancer. *Biochem. Biophys. Res. Commun.* **469,** 985–992 (2016).

29. Liu, X. *et al.* Effects of the suppression of lactate dehydrogenase A on the growth and invasion of human gastric cancer cells. *Oncol. Rep.* **33,** 157–162 (2015).

30. Koukourakis, M. I. *et al.* Lactate dehydrogenase-5 (LDH-5) overexpression in non-small-cell lung cancer tissues is linked to tumour hypoxia, angiogenic factor production and poor prognosis. *Br. J. Cancer* **89,** 877–885 (2003).

31. Koukourakis, M. I., Giatromanolaki, A., Simopoulos, C., Polychronidis, A. & Sivridis, E. Lactate dehydrogenase 5 (LDH5) relates to up-regulated hypoxia inducible factor pathway and metastasis in colorectal cancer. *Clin. Exp. Metastasis* **22,** 25–30 (2005).

32. Koukourakis, M. I. *et al.* Lactate dehydrogenase 5 expression in squamous cell head and neck cancer relates to prognosis following radical or postoperative radiotherapy. *Oncology* **77,** 285–292 (2009).

33. Balkwill, F. & Mantovani, A. Inflammation and cancer: Back to Virchow? *Lancet* **357,** 539–545 (2001).

34. Shalapour, S. & Karin, M. Immunity, inflammation, and cancer: An eternal fight between good and evil. *J. Clin. Invest.* **125,** 3347–3355 (2015).

35. Chang, C. H. *et al.* Posttranscriptional control of T cell effector function by aerobic glycolysis. *Cell* **153,** 1239 (2013).

36. Dietl, K. *et al.* Lactic Acid and Acidification Inhibit TNF Secretion and Glycolysis of Human Monocytes. *J. Immunol.* **184,** 1200–1209 (2010).

37. Palmer, C. S., Ostrowski, M., Balderson, B., Christian, N. & Crowe, S. M. Glucose metabolism regulates T cell activation, differentiation, and functions. *Front. Immunol.* **6,** (2015).

38. O'Sullivan, D., Sanin, D. E., Pearce, E. J. & Pearce, E. L. Metabolic interventions in the immune response to cancer. *Nat. Rev. Immunol.* **19,** 324–335 (2019).

39. Sola-Penna, M. Metabolic regulation by lactate. *IUBMB Life* **60,** 605–608 (2008).

40. Faubert, B. *et al.* Lactate Metabolism in Human Lung Tumors. *Cell* **171,** 358–371.e9 (2017).

41. Walenta, S. & Mueller-Klieser, W. F. Lactate: Mirror and motor of tumor malignancy. *Semin. Radiat. Oncol.* **14,** 267–274 (2004).

42. Brizel, D. M. *et al.* Elevated tumor lactate concentrations predict for an increased risk of metastases in head-and-neck cancer. *Int. J. Radiat. Oncol. Biol. Phys.* **51,** 349–353 (2001).

43. Ziebart, T. *et al.* Metabolic and proteomic differentials in head and neck squamous cell carcinomas and normal gingival tissue. *J. Cancer Res. Clin. Oncol.* **137,** 193–199 (2011).

44. Beckert, S. *et al.* Lactate stimulates endothelial cell migration. *Wound Repair Regen.* **14,** 321–324 (2006).

45. Hunt, T. K., Aslam, R., Hussain, Z. & Beckert, S. Lactate, with oxygen, incites angiogenesis. *Adv. Exp. Med. Biol.* **614,** 73–80 (2008).

46. Hirschhaeuser, F., Sattler, U. G. A. & Mueller-Klieser, W. Lactate: A metabolic key player in cancer. *Cancer Res.* **71,** 6921–6925 (2011).

47. Goetze, K., Walenta, S., Ksiazkiewicz, M., Kunz-Schughart, L. A. & Mueller-Klieser, W. Lactate enhances motility of tumor cells and inhibits monocyte migration and cytokine release. *Int. J. Oncol.* **39,** 453–463 (2011).

48. Halestrap, A. P. The SLC16 gene family-Structure, role and regulation in health and disease. *Mol. Aspects Med.* **34,** 337–349 (2013).

49. Granja, S., Tavares-Valente, D., Queirós, O. & Baltazar, F. Value of pH regulators in the diagnosis, prognosis and treatment of cancer. *Semin. Cancer Biol.* **43,** 17–34 (2017).

50. Parks, S. K., Chiche, J. & Pouysségur, J. Disrupting proton dynamics and energy metabolism for cancer therapy. *Nat. Rev. Cancer* **13,** 611–623 (2013).

51. Pucino, V., Bombardieri, M., Pitzalis, C. & Mauro, C. Lactate at the crossroads of metabolism, inflammation, and autoimmunity. *Eur. J. Immunol.* **47,** 14–21 (2017).

52. Angelin, A. *et al.* Foxp3 Reprograms T Cell Metabolism to Function in Low-Glucose, High-Lactate Environments. *Cell Metab.* **25,** 1282–1293.e7 (2017).

53. Errea, A. *et al.* Lactate inhibits the pro-inflammatory response and metabolic reprogramming in Murine macrophages in a GPR81-independent manner. *PLoS One* **11,** e0163694 (2016).

54. Husain, Z., Huang, Y., Seth, P. & Sukhatme, V. P. Tumor-Derived Lactate Modifies Antitumor Immune Response: Effect on Myeloid-Derived Suppressor Cells and NK Cells. *J. Immunol.* **191,** 1486–1495 (2013).

55. Morrot, A. *et al.* Metabolic symbiosis and immunomodulation: How tumor cell-derived lactate may disturb innate and adaptive immune responses. *Front. Oncol.* **8,** 81 (2018).

56. Tan, Z. *et al.* The monocarboxylate transporter 4 is required for glycolytic reprogramming and inflammatory response in macrophages. *J. Biol. Chem.* **290,** 46–55 (2015).

57. Gottfried, E. *et al.* Tumor-derived lactic acid modulates dendritic cell activation and antigen expression. *Blood* **107,** 2013–2021 (2006).

58. Chirasani, S. R. *et al.* Diclofenac inhibits lactate formation and efficiently counteracts local immune suppression in a murine glioma model. *Int. J. Cancer* **132,** 843–853 (2012).

59. Brand, A. *et al.* LDHA-Associated Lactic Acid Production Blunts Tumor Immunosurveillance by T and NK Cells. *Cell Metab.* **24,** 657–671 (2016).

60. Fischer, K. *et al.* Inhibitory effect of tumor cell-derived lactic acid on human T cells. *Blood* **109,** 3812–3819 (2007).

61. Huber, V. *et al.* Cancer acidity: An ultimate frontier of tumor immune escape and a novel target of immunomodulation. *Semin. Cancer Biol.* **43,** 74–89 (2017).

62. Lacroix, R., Rozeman, E. A., Kreutz, M., Renner, K. & Blank, C. U. Targeting tumor-associated acidity in cancer immunotherapy. *Cancer Immunol. Immunother.* **67,** 1331–1348 (2018).

63. Xia, H. *et al.* Suppression of FIP200 and autophagy by tumor-derived lactate promotes naïve T cell apoptosis and affects tumor immunity. *Sci. Immunol.* **2,** eaan4631 (2017).

64. Ippolito, L., Morandi, A., Giannoni, E. & Chiarugi, P. Lactate: A Metabolic Driver in the Tumour Landscape. *Trends Biochem. Sci.* **44,** 153–166 (2019).

65. Marchiq, I. & Pouysségur, J. Hypoxia, cancer metabolism and the therapeutic benefit of targeting lactate/H+ symporters. *J. Mol. Med.* **94,** 155–171 (2016).

66. Van Ravenswaay Claasen, H. H., Kluin, P. M. & Fleuren, G. J. Tumor infiltrating cells in human cancer: On the possible role of CD16+ macrophages in antitumor cytotoxicity. *Lab. Investig.* **67,** 166–174 (1992).

67. Van Overmeire, E., Laoui, D., Keirsse, J., Van Ginderachter, J. A. & Sarukhan, A. Mechanisms driving macrophage diversity and specialization in distinct tumor microenvironments and parallelisms with other tissues. *Front. Immunol.* **5,** 127 (2014).

68. Mantovani, A., Allavena, P., Sica, A. & Balkwill, F. Cancer-related inflammation. *Nature* **454,** 436–444 (2008).

69. Biswas, S. K. & Mantovani, A. Orchestration of metabolism by macrophages. *Cell Metab.* **15,** 432–437 (2012).

70. Geeraerts, X., Bolli, E., Fendt, S. M. & Van Ginderachter, J. A. Macrophage metabolism as therapeutic target for cancer, atherosclerosis, and obesity. *Front. Immunol.* **8,** 289 (2017).

71. Ginhoux, F. & Jung, S. Monocytes and macrophages: Developmental pathways and tissue homeostasis. *Nat. Rev. Immunol.* **14,** 392–404 (2014).

72. Mills, C. D., Kincaid, K., Alt, J. M., Heilman, M. J. & Hill, A. M. M-1/M-2 Macrophages and the Th1/Th2 Paradigm. *J. Immunol.* **164,** 6166–6173 (2000).

73. Kim, J. Regulation of immune cell functions by metabolic reprogramming. *J. Immunol. Res.* **2018,** (2018).

74. Xue, J. *et al.* Transcriptome-Based Network Analysis Reveals a Spectrum Model of Human Macrophage Activation. *Immunity* **40,** 274–288 (2014).

75. Biswas, S. K. & Mantovani, A. Macrophage plasticity and interaction with lymphocyte subsets: Cancer as a paradigm. *Nat. Immunol.* **11,** 889–896 (2010).

76. Mantovani, A. *et al.* The chemokine system in diverse forms of macrophage activation and polarization. *Trends Immunol.* **25,** 677–686 (2004).

77. Cordes, T. *et al.* Immunoresponsive gene 1 and itaconate inhibit succinate dehydrogenase to modulate intracellular succinate levels. *J. Biol. Chem.* **291,** 14274–14284 (2016).

78. Tannahill, G. M. *et al.* Succinate is an inflammatory signal that induces IL-1β through HIF-1α. *Nature* **496,** 238–242 (2013).

79. Wang, T. *et al.* HIF1 α -Induced Glycolysis Metabolism Is Essential to the Activation of Inflammatory Macrophages. *Mediators Inflamm.* **2017,** 9029327 (2017).

80. Freemerman, A. J. *et al.* Metabolic reprogramming of macrophages: Glucose transporter 1 (GLUT1)-mediated glucose metabolism drives a proinflammatory phenotype. *J. Biol. Chem.* **289,** 7884–7896 (2014).

81. Thapa, B. & Lee, K. Metabolic influence on macrophage polarization and pathogenesis. *BMB Rep.* **52,** 360–372 (2019).

82. Koo, S. jie, Szczesny, B., Wan, X., Putluri, N. & Garg, N. J. Pentose phosphate shunt modulates reactive oxygen species and nitric oxide production controlling Trypanosoma cruzi in Macrophages. *Front. Immunol.* **9,** 202 (2018).

83. Kelly, B. & O'Neill, L. A. J. Metabolic reprogramming in macrophages and dendritic cells in innate immunity. *Cell Res.* **25,** 771–784 (2015).

84. Van den Bossche, J. *et al.* Mitochondrial Dysfunction Prevents Repolarization of Inflammatory Macrophages. *Cell Rep.* **17,** 684–696 (2016).

85. Ghesquière, B., Wong, B. W., Kuchnio, A. & Carmeliet, P. Metabolism of stromal and immune cells in health and disease. *Nature* **511,** 167–176 (2014).

86. Mills, E. L. & O'Neill, L. A. Reprogramming mitochondrial metabolism in macrophages as an anti-inflammatory signal. *Eur. J. Immunol.* **46,** 13–21 (2016).

87. Galván-Peña, S. & O'Neill, L. A. J. Metabolic reprograming in macrophage polarization. *Front. Immunol.* **5,** 420 (2014).

88. Jha, A. K. *et al.* Network integration of parallel metabolic and transcriptional data reveals metabolic modules that regulate macrophage polarization. *Immunity* **42,** 419–430 (2015).

89. Yang, C. *et al.* Glutamine oxidation maintains the TCA cycle and cell survival during impaired mitochondrial pyruvate transport. *Mol. Cell* **56,** 414–424 (2014).

90. Ligthart-Melis, G. C. *et al.* Glutamine is an important precursor for de novo synthesis of arginine in humans. *Am. J. Clin. Nutr.* **87,** 1282–1289 (2008).

91. Palmieri, E. M. *et al.* Pharmacologic or Genetic Targeting of Glutamine Synthetase Skews Macrophages toward an M1-like Phenotype and Inhibits Tumor Metastasis. *Cell Rep.* **20,** 1654–1666 (2017).

92. Zhang, Q. wen *et al.* Prognostic Significance of Tumor-Associated Macrophages in Solid Tumor: A Meta-Analysis of the Literature. *PLoS One* **7,** e50946 (2012).

93. Qian, B. Z. & Pollard, J. W. Macrophage Diversity Enhances Tumor Progression and Metastasis. *Cell* **141,** 39–51 (2010).

94. Murdoch, C., Muthana, M., Coffelt, S. B. & Lewis, C. E. The role of myeloid cells in the promotion of tumour angiogenesis. *Nat. Rev. Cancer* **8,** 618–631 (2008).

95. Kessenbrock, K., Plaks, V. & Werb, Z. Matrix Metalloproteinases: Regulators of the Tumor Microenvironment. *Cell* **141,** 52–67 (2010).

96. Ruffell, B. *et al.* Macrophage IL-10 Blocks CD8+ T Cell-Dependent Responses to Chemotherapy by Suppressing IL-12 Expression in Intratumoral Dendritic Cells. *Cancer Cell* **26,** 623–637 (2014).

97. Krneta, T. *et al.* M2-polarized and tumor-associated macrophages alter NK cell phenotype and function in a contact-dependent manner. *J. Leukoc. Biol.* **101,** 285–295 (2017).

98. Liu, J. *et al.* Tumor-associated macrophages recruit CCR6+ regulatory T cells and promote the development of colorectal cancer via enhancing CCL20 production in mice. *PLoS One* **6,** e19495 (2011).

99. Lesokhin, A. M. *et al.* Monocytic CCR2 + myeloid-derived suppressor cells promote immune escape by limiting activated CD8 T-cell infiltration into the tumor microenvironment. *Cancer Res.* **72,** 876–886 (2012).

100. Movahedi, K. *et al.* Different tumor microenvironments contain functionally distinct subsets of macrophages derived from Ly6C(high) monocytes. *Cancer Res.* **70,** 5728–5739 (2010).

101. Casazza, A. *et al.* Impeding Macrophage Entry into Hypoxic Tumor Areas by Sema3A/Nrp1 Signaling Blockade Inhibits Angiogenesis and Restores Antitumor Immunity. *Cancer Cell* **24,** 695–709 (2013).

102. Park, J. E. *et al.* Hypoxia-induced tumor exosomes promote M2-like macrophage polarization of infiltrating myeloid cells and microRNA-mediated metabolic shift. *Oncogene* **38,** 5158–5173 (2019).

103. Wenes, M. *et al.* Macrophage Metabolism Controls Tumor Blood Vessel Morphogenesis and Metastasis. *Cell Metab.* **24,** 701–715 (2016).

104. Mu, X. *et al.* Tumor-derived lactate induces M2 macrophage polarization via the activation of the ERK/STAT3 signaling pathway in breast cancer. *Cell Cycle* **17,** 428–438 (2018).

105. Colegio, O. R. *et al.* Functional polarization of tumour-associated macrophages by tumour-derived lactic acid. *Nature* **513,** 559–563 (2014).

106. Bronte, V. Tumor cells hijack macrophages via lactic acid. *Immunol. Cell Biol.* **92,** 647–649 (2014).

107. Chen, P. *et al.* Gpr132 sensing of lactate mediates tumor-macrophage interplay to promote breast cancer metastasis. *Proc. Natl. Acad. Sci. U. S. A.* **114,** 580–585 (2017).

108. Ye, H. *et al.* Tumor-associated macrophages promote progression and the Warburg effect via CCL18/NF-kB/VCAM-1 pathway in pancreatic ductal adenocarcinoma. *Cell Death Dis.* **9,** 453 (2018).

109. Zhao, Y. *et al.* Bladder cancer cells re-educate TAMs through lactate shuttling in the microfluidic cancer microenvironment. *Oncotarget* **6,** 39196–39210 (2015).

110. Ohashi, T. *et al.* M2-like macrophage polarization in high lactic acid-producing head and neck cancer. *Cancer Sci.* **108,** 1128–1134 (2017).

111. Halestrap, A. P. & Meredith, D. The SLC16 gene family - From monocarboxylate transporters (MCTs) to aromatic amino acid transporters and beyond. *Pflugers Arch. Eur. J. Physiol.* **447,** 619–628 (2004).

112. Halestrap, A. P. & Price, N. T. The proton-linked monocarboxylate transporter (MCT) family: Structure, function and regulation. *Biochem. J.* **343,** 281–299 (1999).

113. Wilson, M. C. *et al.* Basigin (CD147) is the target for organomercurial inhibition of monocarboxylate transporter isoforms 1 and 4: The ancillary protein for the insensitive MCT2 is embigin (gp70). *J. Biol. Chem.* **280,** 27213–27221 (2005).

114. Romero-Garcia, S., Moreno-Altamirano, M. M. B., Prado-Garcia, H. & Sánchez-García, F. J. Lactate contribution to the tumor microenvironment: Mechanisms, effects on immune cells and therapeutic relevance. *Front. Immunol.* **7,** 52 (2016).

115. Chiche, J. *et al.* In vivo pH in metabolic-defective Ras-transformed fibroblast tumors: Key role of the monocarboxylate transporter, MCT4, for inducing an alkaline intracellular pH. *Int. J. Cancer* **130,** 1511–1520 (2012).

116. Ullah, M. S., Davies, A. J. & Halestrap, A. P. The plasma membrane lactate transporter MCT4, but not MCT1, is up-regulated by hypoxia through a HIF-1α-dependent mechanism. *J. Biol. Chem.* **281,** 9030–9037 (2006).

117. Boidot, R. *et al.* Regulation of monocarboxylate transporter MCT1 expression by p53 mediates inward and outward lactate fluxes in tumors. *Cancer Res.* **72,** 939–948 (2012).

118. Pinheiro, C. *et al.* Role of monocarboxylate transporters in human cancers: State of the art. *J. Bioenerg. Biomembr.* **44,** 127–139 (2012).

119. Brooks, G. A. The Science and Translation of Lactate Shuttle Theory. *Cell Metab.* **27,** 757–785 (2018).

120. Stanley, W. C., Wisneski, J. A., Gertz, E. W., Neese, R. A. & Brooks, G. A. Glucose and lactate interrelations during moderate-intensity exercise in humans. *Metabolism* **37,** 850–858 (1988).

121. Magistretti, P. J. & Pellerin, L. Cellular Bases of Brain Energy Metabolism and Their Relevance to Functional Brain Imaging: Evidence for a Prominent Role of Astrocytes. *Cereb. Cortex* **6,** 50–61 (1996).

122. Skelton, M. S., Kremer, D. E., Smith, E. W. & Gladden, L. B. Lactate influx into red blood cells of athletic and nonathletic species. *Am. J. Physiol. - Regul. Integr. Comp. Physiol.* **268,** R1121-8 (1995).

123. Bergersen, L. H. Is lactate food for neurons? Comparison of monocarboxylate transporter subtypes in brain and muscle. *Neuroscience* **145,** 11–19 (2007).

124. Sonveaux, P. *et al.* Targeting lactate-fueled respiration selectively kills hypoxic tumor cells in mice. *J. Clin. Invest.* **118,** 3930–3942 (2008).

125. Rademakers, S. E., Lok, J., van der Kogel, A. J., Bussink, J. & Kaanders, J. H. A. M. Metabolic markers in relation to hypoxia; staining patterns and colocalization of pimonidazole, HIF-1α, CAIX, LDH-5, GLUT-1, MCT1 and MCT4. *BMC Cancer* **11,** 167 (2011).

126. Pérez-Escuredo, J. *et al.* Monocarboxylate transporters in the brain and in cancer. *Biochim. Biophys. Acta - Mol. Cell Res.* **1863,** 2481–2497 (2016).

127. Végran, F., Boidot, R., Michiels, C., Sonveaux, P. & Feron, O. Lactate influx through the endothelial cell monocarboxylate transporter MCT1 supports an NF-kB/IL-8 pathway that drives tumor angiogenesis. *Cancer Res.* **71,** 2550–2560 (2011).

128. Tao, L., Huang, G., Song, H., Chen, Y. & Chen, L. Cancer associated fibroblasts: An essential role in the tumor microenvironment (review). *Oncol. Lett.* **14,** 2611–2620 (2017).

129. Pavlides, S. *et al.* The reverse Warburg effect: Aerobic glycolysis in cancer associated fibroblasts and the tumor stroma. *Cell Cycle* **8,** 3984–4001 (2009).

130. Whitaker-Menezes, D. *et al.* Evidence for a stromal-epithelial 'lactate shuttle' in human tumors: MCT4 is a marker of oxidative stress in cancer-associated fibroblasts. *Cell Cycle* **10,** 1772–1783 (2011).

131. Chang, C. H. & Pearce, E. L. Emerging concepts of T cell metabolism as a target of immunotherapy. *Nat. Immunol.* **17,** 364–368 (2016).

132. Chang, C. H. *et al.* Metabolic Competition in the Tumor Microenvironment Is a Driver of Cancer Progression. *Cell* **162,** 1229–1241 (2015).

133. Wang, T., Liu, G. & Wang, R. The intercellular metabolic interplay between tumor and immune cells. *Front. Immunol.* **5,** 538 (2014).

134. Morais-Santos, F. *et al.* Targeting lactate transport suppresses in vivo breast tumour growth. *Oncotarget* **6,** 19177–19189 (2015).

135. Gallagher, S. M., Castorino, J. J., Wang, D. & Philp, N. J. Monocarboxylate transporter 4 regulates maturation and trafficking of CD147 to the plasma membrane in the metastatic breast cancer cell line MDA-MB-231. *Cancer Res.* **67,** 4182–4189 (2007).

136. Doherty, J. R. & Cleveland, J. L. Targeting lactate metabolism for cancer therapeutics. *J. Clin. Invest.* **123,** 3685–3692 (2013).

137. Mathupala, S. P., Parajuli, P. & Sloan, A. E. Silencing of monocarboxylate transporters via small interfering ribonucleic acid inhibits glycolysis and induces cell death in malignant glioma: An in vitro study. *Neurosurgery* **55,** 1410–1419 (2004).

138. Nancolas, B. *et al.* The anti-tumour agent lonidamine is a potent inhibitor of the mitochondrial pyruvate carrier and plasma membrane monocarboxylate transporters. *Biochem. J.* **473,** 929–936 (2016).

139. Colen, C. B. *et al.* Metabolic remodeling of malignant gliomas for enhanced sensitization during radiotherapy: An in vitro study. *Neurosurgery* **59,** 1313–1323 (2006).

140. Morais-Santos, F. *et al.* Differential sensitivities to lactate transport inhibitors of breast cancer cell lines. *Endocr. Relat. Cancer* **21,** 27–38 (2014).

141. Halestrap, A. P. The monocarboxylate transporter family-Structure and functional characterization. *IUBMB Life* **64,** 1–9 (2012).

142. Ovens, M. J., Davies, A. J., Wilson, M. C., Murray, C. M. & Halestrap, A. P. AR-C155858 is a potent inhibitor of monocarboxylate transporters MCT1 and MCT2 that binds to an intracellular site involving transmembrane helices 7-10. *Biochem. J.* **425,** 523–530 (2010).

143. Guan, X., Rodriguez-Cruz, V. & Morris, M. E. Cellular Uptake of MCT1 Inhibitors AR-C155858 and AZD3965 and Their Effects on MCT-Mediated Transport of L-Lactate in Murine 4T1 Breast Tumor Cancer Cells. *AAPS J.* **21,** 13 (2019).

144. Curtis, N. J. *et al.* Pre-clinical pharmacology of AZD3965, a selective inhibitor of MCT1: DLBCL, NHL and Burkitt's lymphoma anti-tumor activity. *Oncotarget* **8,** 69219–69236 (2017).

145. Bola, B. M. *et al.* Inhibition of monocarboxylate transporter-1 (MCT1) by AZD3965 enhances radiosensitivity by reducing lactate transport. *Mol. Cancer Ther.* **13,** 2805–2816 (2014).

146. Polanski, R. *et al.* Activity of the Monocarboxylate Transporter 1 Inhibitor AZD3965 in Small Cell Lung Cancer. *Clin. Cancer Res.* **20,** 926–937 (2014).

147. Beloueche-Babari, M. *et al.* MCT1 inhibitor AZD3965 increases mitochondrial metabolism, facilitating combination therapy and noninvasive magnetic resonance spectroscopy. *Cancer Res.* **77,** 5913–5924 (2017).

148. Le Floch, R. *et al.* CD147 subunit of lactate/H+ symporters MCT1 and hypoxia-inducible MCT4 is critical for energetics and growth of glycolytic tumors. *Proc. Natl. Acad. Sci. U. S. A.* **108,** 16663–16668 (2011).

149. Ždralević, M. *et al.* Disrupting the 'Warburg effect' re-routes cancer cells to OXPHOS offering a vulnerability point via 'ferroptosis'-induced cell death. *Adv. Biol. Regul.* **68,** 55–63 (2018).

150. Bertram, J. S. & Janik, P. Establishment of a cloned line of Lewis lung carcinoma cells adapted to cell culture. *Cancer Lett.* **11,** 63–73 (1980).

151. Sirotnak, F. M., DeGraw, J. I., Schmid, F. A., Goutas, L. J. & Moccio, D. M. New folate analogs of the 10-deaza-aminopterin series - Further evidence for markedly increased antitumor efficacy compared with methotrexate in ascitic and solid murine tumor models. *Cancer Chemother. Pharmacol.* **12,** 26–30 (1984).

152. Gstraunthaler, G. Alternatives to the use of fetal bovine serum: serum-free cell culture. *ALTEX Altern. zu Tierexperimenten* **20,** 275–281 (2003).

153. Martínez-Liarte, J. H., Solano, F. & Lozano, J. A. Effect of Penicillin-Streptomycin and Other Antibiotics on Melanogenic Parameters in Cultured B16/F10 Melanoma Cells. *Pigment Cell Res.* **8,** 83–88 (1995).

154. Martinez-Lage, M., Puig-Serra, P., Menendez, P., Torres-Ruiz, R. & Rodriguez-Perales, S. CRISPR/Cas9 for cancer therapy: Hopes and challenges. *Biomedicines* **6,** 105 (2018).

155. Bradford, M. M. A rapid and sensitive method for the quantitation of microgram quantities of protein utilizing the principle of protein-dye binding. *Anal. Biochem.* **72,** 248–254 (1976).

156. Kuete, V., Karaosmanoğlu, O. & Sivas, H. Anticancer Activities of African Medicinal Spices and Vegetables. in *Medicinal Spices and Vegetables from Africa: Therapeutic Potential Against Metabolic, Inflammatory, Infectious and Systemic Diseases* 271–297 (2017).

157. Giandomenico, A. R., Cerniglia, G. E., Biaglow, J. E., Stevens, C. W. & Koch, C. J. The importance of sodium pyruvate in assessing damage produced by hydrogen peroxide. *Free Radic. Biol. Med.* **23,** 426–434 (1997).

158. Kim, H. Glutamine as an immunonutrient. *Yonsei Med. J.* **52,** 892–897 (2011).

159. Baicu, S. C. & Taylor, M. J. Acid-base buffering in organ preservation solutions as a function of

temperature: New parameters for comparing buffer capacity and efficiency. *Cryobiology* **45,** 33–48 (2002).

160. Englen, M. D., Valdez, Y. E., Lehnert, N. M. & Lehnert, B. E. Granulocyte/macrophage colony-stimulating factor is expressed and secreted in cultures of murine L929 cells. *J. Immunol. Methods* **184,** 281–283 (1995).

161. Stanley, E. R. *et al.* Biology and action of colony-stimulating factor-1. *Mol. Reprod. Dev.* **46,** 4–10 (1997).

162. Hu, X., Chao, M. & Wu, H. Central role of lactate and proton in cancer cell resistance to glucose deprivation and its clinical translation. *Signal Transduct. Target. Ther.* **2,** 16047 (2017).

163. Mason, P. E., Neilson, G. W., Dempsey, C. E., Barnes, A. C. & Cruickshank, J. M. The hydration structure of guanidinium and thiocyanate ions: Implications for protein stability in aqueous solution. *Proc. Natl. Acad. Sci. U. S. A.* **100,** 4557–4561 (2003).

164. Nolan, T., Hands, R. E. & Bustin, S. A. Quantification of mRNA using real-time RT-PCR. *Nat. Protoc.* **1,** 1559–1582 (2006).

165. Veiga, S. R. *et al.* Phenformin-induced mitochondrial dysfunction sensitizes hepatocellular carcinoma for dual inhibition of mTOR. *Clin. Cancer Res.* **24,** 3767–3780 (2018).

166. Hanahan, D. & Weinberg, R. A. The hallmarks of cancer. *Cell* **100,** 57–70 (2000).

167. Holness, C. L. & Simmons, D. L. Molecular cloning of CD68, a human macrophage marker related to lysosomal glycoproteins. *Blood* **81,** 1607–1613 (1993).

168. Wang, R. *et al.* Tumor-associated macrophages provide a suitable microenvironment for non-small lung cancer invasion and progression. *Lung Cancer* **74,** 188–196 (2011).

169. Yang, J., Li, X., Liu, X. P. & Liu, Y. The role of tumor-associated macrophages in breast carcinoma invasion and metastasis. *Int. J. Clin. Exp. Pathol.* **8,** 6656–6664 (2015).

170. Chen, J. J. W. *et al.* Up-regulation of tumor interleukin-8 expression by infiltrating macrophages: Its correlation with tumor angiogenesis and patient survival in non-small cell lung cancer. *Clin. Cancer Res.* **9,** 729–737 (2003).

171. Urs, S. E0771 Syngeneic Breast Cancer Model. (2018). Available at: https://www.mibioresearch.com/knowledge-center/e0771-syngeneic-breast-cancer-model/.

172. Granja, S. *et al.* Disruption of BASIGIN decreases lactic acid export and sensitizes non-small cell lung cancer to biguanides independently of the LKB1 status. *Oncotarget* **6,** 6708–6721 (2015).

173. Marchiq, I., Le Floch, R., Roux, D., Simon, M. P. & Pouyssegur, J. Genetic disruption of lactate/H+ symporters (MCTs) and their subunit CD147/BASIGIN sensitizes glycolytic tumor cells to phenformin. *Cancer Res.* **75,** 171–180 (2015).

174. Hong, C. S. *et al.* MCT1 Modulates Cancer Cell Pyruvate Export and Growth of Tumors that Co-express MCT1 and MCT4. *Cell Rep.* **14,** 1590–1601 (2016).

175. Doherty, J. R. *et al.* Blocking lactate export by inhibiting the myc target MCT1 disables glycolysis and glutathione synthesis. *Cancer Res.* **74,** 908–920 (2014).

176. Lin, S. *et al.* Lactate-activated macrophages induced aerobic glycolysis and epithelial-mesenchymal transition in breast cancer by regulation of CCL5-CCR5 axis: A positive metabolic feedback loop. *Oncotarget* **8,** 110426–110443 (2017).

177. Schmall, A. *et al.* Macrophage and cancer cell cross-talk via CCR2 and CX3CR1 is a fundamental mechanism driving lung cancer. *Am. J. Respir. Crit. Care Med.* **191,** 437–447 (2015).

178. Madera, L., Greenshields, A., Coombs, M. R. P. & Hoskin, D. W. 4T1 Murine Mammary Carcinoma Cells Enhance Macrophage-Mediated Innate Inflammatory Responses. *PLoS One* **10,** e0133385 (2015).

179. Kimura, Y. N. *et al.* Inflammatory stimuli from macrophages and cancer cells synergistically promote tumor growth and angiogenesis. *Cancer Sci.* **98,** 2009–2018 (2007).

180. Caldwell, R. B., Toque, H. A., Narayanan, S. P. & Caldwell, R. W. Arginase: An old enzyme with new tricks. *Trends Pharmacol. Sci.* **36,** 395–405 (2015).

181. Wei, C. *et al.* Crosstalk between cancer cells and tumor associated macrophages is required for mesenchymal circulating tumor cell-mediated colorectal cancer metastasis. *Mol. Cancer* **18,** (2019).

182. Penny, H. L. *et al.* Warburg metabolism in tumor-conditioned macrophages promotes metastasis in human pancreatic ductal adenocarcinoma. *Oncoimmunology* **5,** (2016).

183. Venkatesh, K. V, Darunte, L. & Bhat, P. J. Warburg Effect. in *Encyclopedia of Systems Biology* (eds. Dubitzky, W., Wolkenhauer, O., Cho, K.-H. & Yokota, H.) 2349–2350 (Springer New York, 2013).

184. Kim, J. A. & Yeom, Y. Il. Metabolic signaling to epigenetic alterations in cancer. *Biomol. Ther.* **26,** 69–80 (2018).